Cloud Parametrization

Adrian M. Tompkins

Abdus Salam International Centre for Theoretical Physics (ICTP),
Strada Costiera 11, Trieste 34000, Italy
tompkins@ictp.it

1 Introduction

Let us introduce the seminar series on subgrid-scale parametrization by examining the progress in the ECMWF forecast system at representing the top-of-atmosphere (TOA) longwave radiation budget. Figure 1 compares an ensemble of year-long integrations using the ECMWF integrated forecasting system forced by observed sea surface temperatures. The left set of panels shows an integration using model cycle 23r4, which was operational in 2000, and was used conduct the ERA-40 reanalysis. The right set of panels shows an integration with cycle CY33R1, operational in 2008[1]. Over the eight intermediate years the errors have been greatly reduced, with the global mean RMS error reduced by almost one half. While some of this error reduction undoubtedly derives from improvements in the large-scale model dynamics and advection, much of it is a result of better subgrid-scale schemes to represent the processes of convection, clouds and cloud-radiation interaction. If the convection scheme produces too little activity over the Tropical American and African continents, as it did in earlier model versions, then it is extremely difficult to adjust cloud scheme tuning parameters to eradicate the IR error. Likewise, if the cloud scheme microphysics allow too much ice to sediment out of tropical cirrus clouds, adjusting the radiative properties of the ice crystals will likely lead to increased errors elsewhere, such as low ice clouds over the poles. Perfect cloud properties of cloud cover and condensate amount will still result in radiative errors if the assumed radiative properties or vertical overlap of those clouds are poor. It is clear that small errors in the TOA IR budgets and other cloud related fields can only result from a harmonious improvement of all subgrid-scale processes, and the 2008 ECMWF seminar series aims to introduce some of the advances that have occurred recently.

This lecture concerns itself with the representation of cloud physics, and these lecture notes draw heavily on (and even duplicate some of) the ECMWF training course lecture notes of Tompkins (2005). When considering the approach to model clouds in general circulation models (GCMs), there are a number of zero order issues that require attention, in addition to the representation of the complex warm phase and ice phase microphysics processes that govern the growth and evolution of cloud and precipitation particles.

Unlike cloud resolving models (CRMs) or large-eddy models (LEMs), which, having grid resolutions finer than O(1km), aim to resolve the motions relevant for the clouds under consideration, GCMs must additionally consider macroscopic geometrical effects. Claiming to resolve cloud scale motions allows CRMs and LEMs to make the assumption that each grid scale is completely cloudy if condensate is present. This approach is clearly not adequate for GCM size grid scale of O(100km) for which clouds are a subgrid-scale phenomenon, (although some schemes such as Ose, 1993; Fowler et al., 1996, have indeed adopted this approach).

GCMs must therefore consider cloud geometrical effects. To reduce the fractal cloud to a tractable low dimensional object, GCMs usually reduce the problem to the specification of the:

[1]The comparison is not entirely "clean" or fair, since the 23r4 integration was performed when the PA section used a 3-member ensemble all initialized at 12Z, the right hand panel uses a 4 member ensemble initialized at 6 hourly intervals, but this impact is minimal for an accumulated flux field such as the TOA IR budget. The astute reader will also note a small change in the observational dataset due to a change in the choice of CERES platform. Both of these differences are minimal and the vast majority of the reduction in the error maps is due to model physics improvements

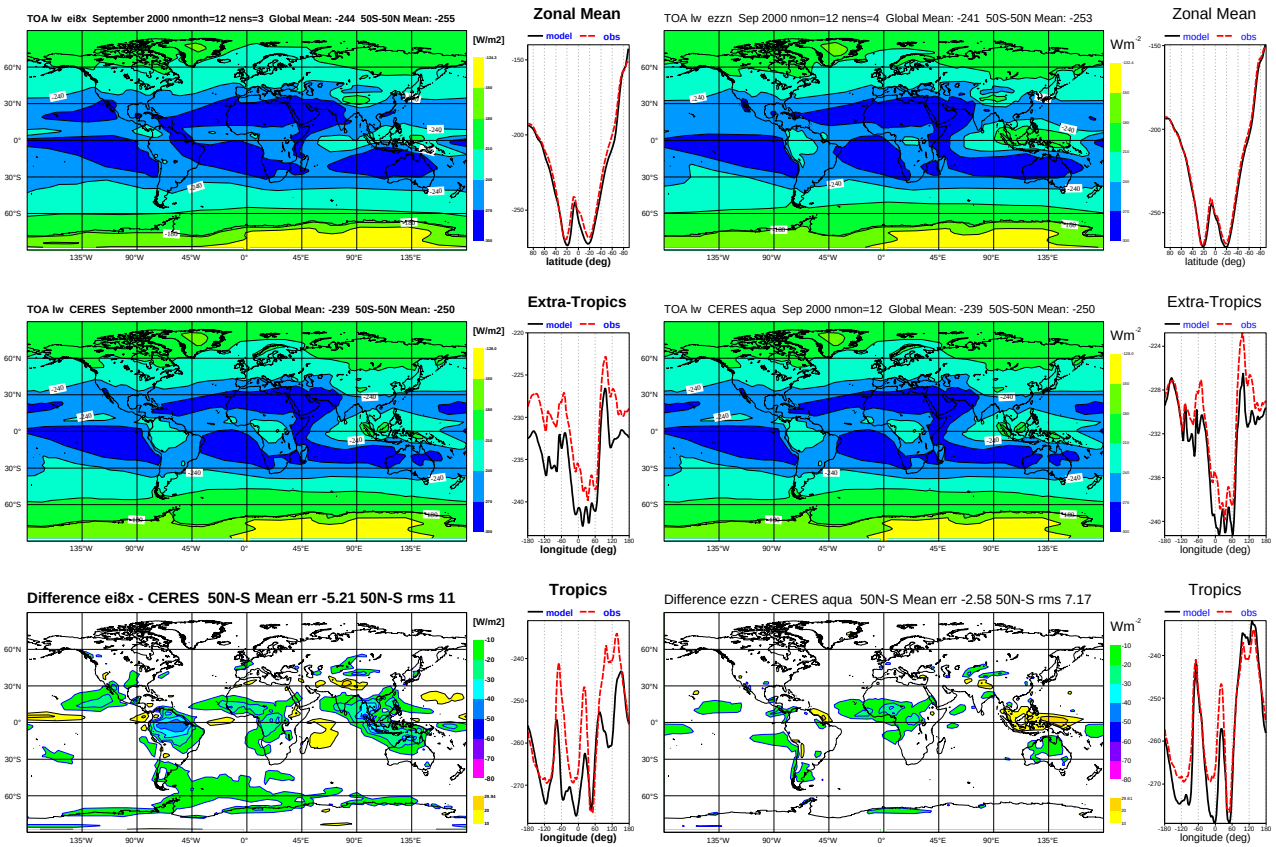

Figure 1: Comparison of ensemble mean net TOA OLR budgets from 13 month integrations of the ECMWF IFS model (top) to CERES observations (middle), with the model-obs difference shown in the lower panels. The left column is for cycle 23R4 while the right for 33R1. The comparison is made for 13-month integrations starting Aug 2000 with the first month discarded.

- horizontal fractional coverage of the gridbox by cloud,
- vertical fractional coverage of the gridbox by cloud,
- sub-cloud variability of cloud variables in both the horizontal and vertical, and the
- overlap of the clouds in the vertical column.

The above list is far from exhaustive, and implicitly neglects interactions between adjacent GCM columns (for example, how cloud affects solar fluxes in adjacent columns at low sun angles), probably a safe assumption for grid-scales exceeding 10km or so (Di Giuseppe and Tompkins, 2003)

In fact, most GCMs further simplify the above list (i) by assuming clouds fill GCM grid boxes in the vertical and (ii) by neglecting many of the consequences of sub-cloud fluctuations of cloud properties. Both of these are considerable simplifications. Although vertical GCM grids are much finer than the horizontal resolution, the same is of course also true of cloud processes. Using O(50) levels in the vertical implies that some cloud systems or microphysical related processes are barely if at all resolved, such as tropical thin cirrus (Dessler and Yang, 2003), or the precipitation melting layer (Kitchen et al., 1994), which can have important implications (Tompkins and Emanuel, 2000). Likewise, many authors have highlighted the biases that can be introduced when sub-cloud fluctuations are neglected, due to the strong nonlinearity of cloud and radiative processes (Cahalan et al., 1994; Barker et al., 1999; Pincus and Klein, 2000; Pomroy and Illingworth, 2000; Fu et al., 2000; Rotstayn, 2000; Larson et al., 2001).

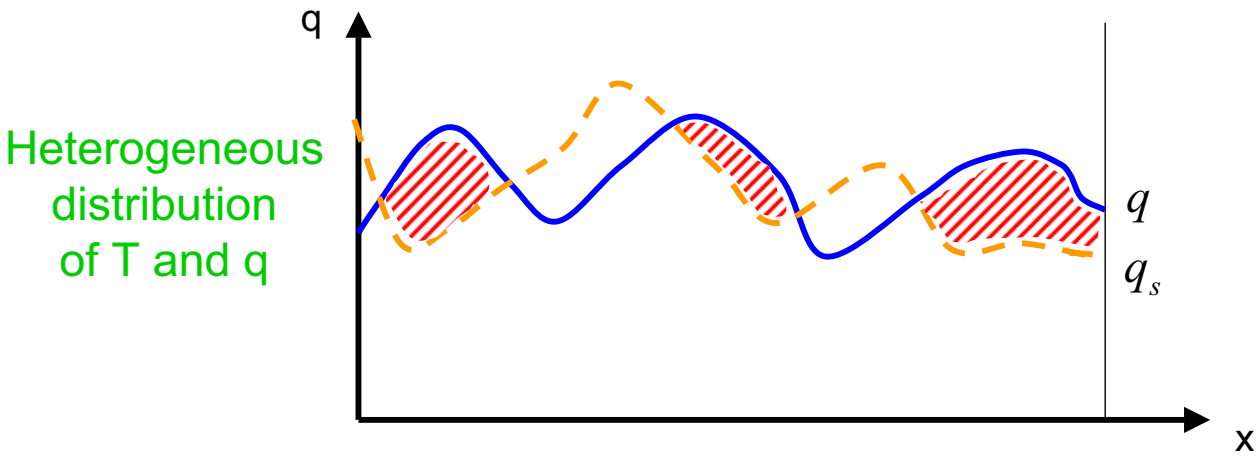

Figure 2: Schematic showing that partial cloud cover in a gridbox in only possible if temperature or humidity fluctuations exist. The blue line shoes humidity and the yellow line saturation mixing ratio across an arbitrary line representing a gridbox. If all supersaturation condenses as cloud then the shaded regions will be cloudy.

Nevertheless, the zero order primary task of cloud schemes, in addition to representing the microphysics of clouds, is to predict the horizontal cloud coverage. It is clear that a Utopian perfect microphysical model will render poor results if combined with an inaccurate predictor of cloud cover, due to the incorrect estimate of in-cloud liquid water.

The equally important issue of cloud microphysics is covered in detail in a complementary lecture by Richard Forbes, and this presentation will mostly concentrate on the issue of cloud geometry and the parametrization of cloud cover.

2 Fractional cloud cover

The first thing to realize is that fractional cloud cover can *only* occur if there is horizontal subgrid-scale variability in humidity and/or temperature (controlling the saturation mixing ratio, q_s)[2]. If temperature and humidity are homogeneous, then either the whole grid box is sub-saturated and clear, or supersaturated and cloudy[3].

This is illustrated schematically in Fig. 2. Fluctuations in temperature and humidity may cause the humidity to exceed the saturated value on the subgrid scale. If it is assumed that all this excess humidity is immediately converted to cloud water (and likewise that any cloud drops evaporate instantly in sub-saturated conditions), then it is clear that the grid-mean relative humidity ($\overline{RH}$, where the overline represents the gridbox average) must be less than unity if the cloud cover is also less than unity, since within the cloudy parts of the gridbox $RH = 1$ and in the clear sky $RH < 1$. Generally speaking, since clouds are unlikely when the atmosphere is dry, and since RH is identically 1 when $C = 1$, there is likely to be a positive correlation between RH and C.

The main point to emphasize is that, *all* cloud schemes that are able to diagnose non-zero cloud cover for $\overline{RH} < 1$ (i.e. any scheme other than an "all-or-nothing" scheme) must make an assumption concerning the fluctuations of humidity and/or temperature on the subgrid-scale, as in Fig. 2. Either (i) they will *explicitly*

[2]As this document replicates figures and is drawn from a variety of sources, the notation for mass mixing ratio intermittently interchanges between r and q. Note that in the literature, while q is commonly used for mass mixing ratio, most textbooks adhere to the convention that q represents the closely-related specific humidity

[3]For simplicity, throughout this initial text we ignore the subtle complication of the ice phase, where super-saturation are common (Heymsfield et al., 1998; Gierens et al., 2000; Spichtinger et al., 2003)

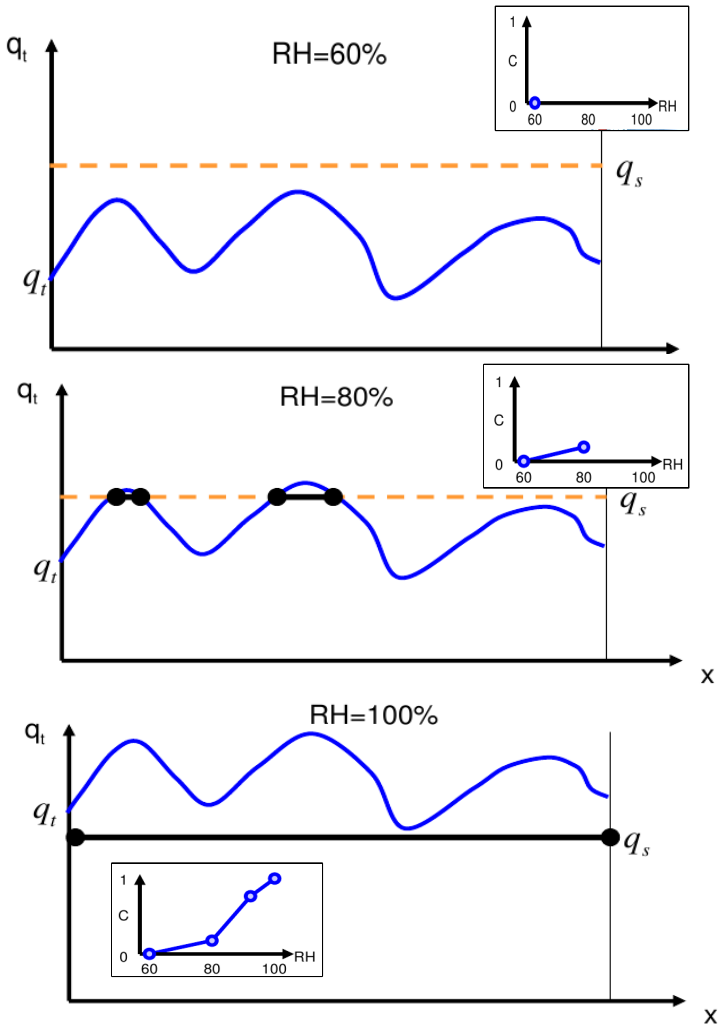

Figure 3: Schematic of RH based scheme, see text for details.

give the nature of these fluctuations, most usually by specifying the probability density function (PDF) for the total water at each gridcell, or (ii) they will *implicitly* assume knowledge about the time-mean statistics of the fluctuations (i.e. the actual PDF at each grid point is maybe not known).

It is important to recall, when trying to categorize the seemingly diverse approaches to cloud cover parametrization, that *this central fact ties all approaches together.*

3 Relative humidity schemes

Relative humidity schemes are called such because they specify a diagnostic relationship between the cloud cover and the relative humidity. In the last section we saw that subgrid-scale fluctuations allow cloud to form when $\overline{RH} < 1$. *RH* schemes formalise this by setting a critical *RH* (denoted RH_{crit}) at which cloud is assumed to form, and then increase *C* according to a monotonically increasing function of *RH*, with *C*=1 identically when *RH*=1. This is illustrated schematically in Fig. 3. In the upper panel a situation is depicted where the mean relative humidity is low, thus even with subgrid-scale fluctuations present, no point in the domain is saturated and therefore cloudy. Given a certain fixed variability, increasing the mean relative humidity implies that a critical threshold is reached at which cloud forms (middle panel), until eventually full saturation and overcast conditions are achieved (lower panel).

In each panel the insert shows the schematic progression of the *RH*-cloud cover relationship. One can therefore specify a monotonically increasing function to describe the increase of cloud cover with *RH* without necessarily knowing the nature or magnitude of the subgrid-scale thermodynamic variability. One commonly used function was given by Sundqvist et al. (1989):

$$C = 1 - \sqrt{\frac{1 - RH}{1 - RH_{crit}}}. \tag{1}$$

It is apparent that RH_{crit} defines the magnitude of the fluctuations of humidity (the humidity variance). If RH_{crit} is small, then the subgrid humidity fluctuations must be large, since cloud can form in mean-dry conditions.

It is clear that one of the drawbacks of this type of scheme is that the link between cloud cover and local dynamical conditions is vague. Convection will indeed produce cloud if its local moistening effect is sufficient to increase *RH* past the critical threshold, but it is apparent that a grid cell with 80% *RH* undergoing deep convection is likely to have different cloud characteristics than a gridcell with 80% *RH* in a frontal stratus cloud. *RH* schemes simply state that, averaged across all conditions across the globe, a gridcell with X% *RH* will have Y% cloud cover.

This lack of differentiation between different local conditions lead some authors to augment their *RH* schemes. The ECHAM4 climate model Roeckner et al. (1996) augments the cloud cover in the presence of a strong temperature inversion to improve the representation of stratocumulus.

Other authors augment their schemes by using additional predictors to *RH*. The Slingo (1980, 1987) scheme was used operationally in the ECMWF forecast model until its replacement by the Tiedtke (1993) scheme in 1995, and was used for a further 10 years in the Tangent linear and adjoint computations of the 4D-Var inner-loops until replaced by Tompkins and Janisková (2004). The basic form for the mid-level cloud cover (C_{mid}) is given as

$$C^*_{mid} = \left(\frac{RH - RH_{crit}}{1 - RH_{crit}} \right)^2, \tag{2}$$

but Slingo modifies this according to an additional predictor, the vertical velocity at 500 hPa (ω_{500}), thus

$$C_{mid} = C^*_{mid} \frac{\omega_{500}}{\omega_{crit}}, \tag{3}$$

if $0 > \omega_{500} > \omega_{crit}$ while the cloud cover is set to zero if subsidence is occurring ($\omega_{500} > 0$).

Xu and Randall (1996) used a cloud resolving model (CRM) to derive an empirical relationship for cloud cover based on the two predictors of *RH* and cloud water content:

$$C = RH^p \left[1 - exp \left(\frac{-\alpha_0 \overline{q_l}}{(q_s - q_v)^\gamma} \right) \right], \tag{4}$$

where γ, α_0 and p are 'tunable' constants of the scheme, with values chosen using the CRM data. One weakness of such a scheme is, of course, this dependence on the reliability of the CRM's parametrizations, in particular the microphysics scheme. Additionally, it is unlikely that the limited set of (convective) cases used as the training dataset would encompass the full range of situations that can naturally arise, such as cloud in frontal systems for example.

While these latter schemes use additional predictors for cloud cover, we shall still refer to them as "relative humidity" schemes, since the common and central predictor in all cases is *RH*. It is doubtful if any of the schemes could be reasonably simplified by replacing the *RH* dependence with a fixed value.

4 Statistical schemes

Instead of describing the spatial and temporal mean statistics of the humidity fluctuations such as the *RH* schemes, another group of schemes take a different approach, *by specifying the underlying distribution of*

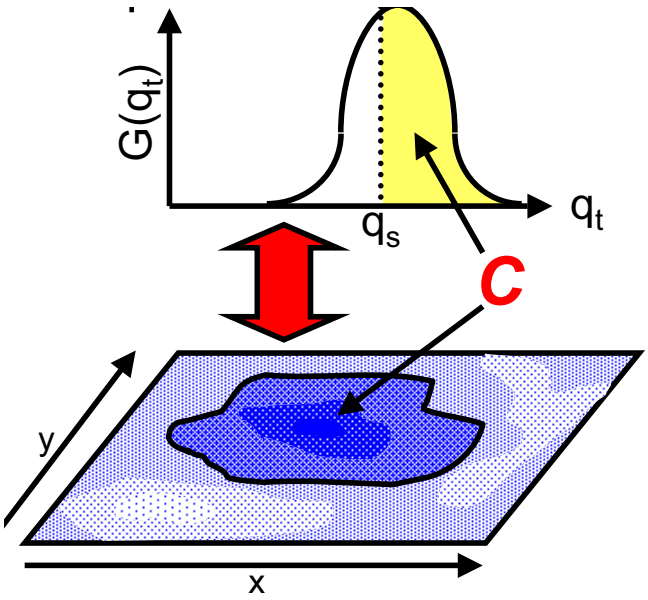

Figure 4: Schematic showing the statistical scheme approach. Upper panel shows an idealized PDF of total water (q_t). The vertical line represents the saturation mixing ratio $q_t = q_s$, thus all the points under the PDF to the right of this line are cloudy. The integral of this area translates to the cloudy portion of the gridbox, marked on the lower part of the figure, with darker shading schematically representing high total water values.

humidity (and/or temperature) variability at each grid box. This is shown schematically in Fig. 4. If the PDF form for total water q_t is known, then the cloud cover C is simply the integral over the part of the PDF for which q_t exceeds q_s:

$$C = \int_{q_s}^{\infty} G(q_t) dq_t . \tag{5}$$

Likewise, the cloud condensate is given by

$$\bar{q_c} = \int_{q_s}^{\infty} (q_t - q_s) G(q_t) dq_t . \tag{6}$$

As always we are assuming that all supersaturation is immediately condensed as cloud. Here we are also ignoring temperature fluctuations for simplicity, but these can be included, as outlined later in this section.

The main tasks of the statistic scheme is therefore to give a suitable form for the PDF of total water fluctuations, and to derive its defining moments.

4.1 Defining the PDF

Various distributions have been used, many of which are symmetrical. Smith (1990) uses a symmetric triangular PDF, diagnosing the variance based on a critical *RH* function at which cloud is determined to form, later modified by Cusack et al. (1999). This PDF has been subsequently adopted by Rotstayn (1997) and Nishizawa (2000). LeTreut and Li (1991) use a uniform distribution, setting the distribution's variance to an arbitrarily defined constant. A Gaussian-like symmetrical polynomial function was used by Lohmann et al. (1999) with variance determined from the subgrid-scale turbulence scheme following Ricard and Royer (1993), who investigated Gaussian, exponential and skewed PDF forms. Bechtold et al. (1992) based their scheme on the Gaussian distribution, which was modified in Bechtold et al. (1995) to a PDF linearly interpolated between Gaussian and exponential distributions. Bony and Emanuel (2001) have introduced a scheme that uses a generalized Log-Normal distribution. Lewellen and Yoh (1993) detail a parameterization that uses a Bi-normal distribution that

Table 1: PDF forms used in statistical cloud schemes. In the summary column, the key is: U=unimodal, B=Bimodal, S=Symmetric, Sk=Skewed.

PDF Shape	Summary	Reference
Double Delta	U,S	Ose (1993); Fowler et al. (1996)
Uniform	U,S	LeTreut and Li (1991)
Triangular	U,S	Smith (1990); Rotstayn (1997); Nishizawa (2000)
Polynomial	U,S	Lohmann et al. (1999)
Gaussian	U,S	Bougeault (1981); Ricard and Royer (1993); Bechtold et al. (1995)
Beta	U,sk	Tompkins (2002)
Log-normal	U,sk	Bony and Emanuel (2001)
Exponential	U,Sk	Bougeault (1981); Ricard and Royer (1993); Bechtold et al. (1995)
Double Gaussian/Normal	B,Sk	Lewellen and Yoh (1993); Golaz et al. (2002)

can be skewed as well as symmetrical and is bimodal, although a number of simplifying assumptions were necessary in order to make the scheme tractable. Likewise Golaz et al. (2002) also give a bimodal scheme. These forms are summarized in table 1.

Examples of PDFs measured in the literature are shown in Figs. 5 and 6 . Although it is difficult to theoretically derive a PDF form, since the q_t distribution is the result of a large number of interacting processes, therefore forcing the use of empirical methods, it is possible to use physically-based arguments to justify certain functional forms. For example, in the absence of other processes, large-scale dynamical mixing would tend to reduce both the variance and the asymmetry the distribution. Therefore, the Gamma and Lognormal distributions would be difficult to use since they are always positively skewed, and only tend to a symmetrical distributions as one of their defining parameters approaches infinity. Bony and Emanuel (2001) attempt to circumnavigate this by switching between Lognormal and Gaussian functions at a threshold skewness value.

Another problem that distributions such as the Lognormal, Gamma, Gaussian and Exponential suffer from is that they are all unbounded functions. Thus, if these functional forms are used, the maximum cloud condensate mixing ratio approaches infinity, and part of the grid cell is always covered by cloud. Precautionary measures, such as the use of a truncated function, can be taken, but this increases the number of parameters required to describe the distribution, and again introduces undesirable discreteness. Moreover, functions such as the Gaussian function or the polynomial used by Lohmann et al. (1999) are also negatively unbounded, implying that part of the gridcell has negative water mass. The choice of function must also involve a fair degree of pragmatism, since in addition to providing a good fit to the available data, it must also be sufficiently simple and of few enough degrees of freedom to be of use in a parameterization scheme. For example, Larson et al. (2001) were able to provide good fits to their aircraft data using a 5-parameter double Gaussian function, but it is unclear how these parameters would be determined in a GCM cloud scheme. The Beta distribution used by Tompkins (2002) is bounded and can provide both symmetrical and skewed distributions, but has the disadvantage of an upper limit on the skewness when the distribution is restricted to a sensible bell-shaped regime, and that the form is not mathematically as simple as alternative unimodal distributions.

Considering the question of whether a unimodal distribution is adequate, we refer to a number of observational studies. Some of the data from the following studies is shown for illustrative purposes in Fig. 5. Ek and Mahrt (1991) examined PBL relative humidity variability in a limited number of flight legs, and assumed a unimodal Gaussian fit for their distribution. Wood and Field (2000) studied flight data from both warm and cold clouds and reported unimodal distributions of q_t, but also observing more complex distributions, giving some weakly and strongly bimodal examples. Davis et al. (1996) reported uni- or bi-modal skewed distributions in liquid water content from flight data in marine stratocumulus clouds. Larson et al. (2001) have also examined flight data for PBL clouds and found that mainly unimodal or bimodal distributions occurred. They reported that

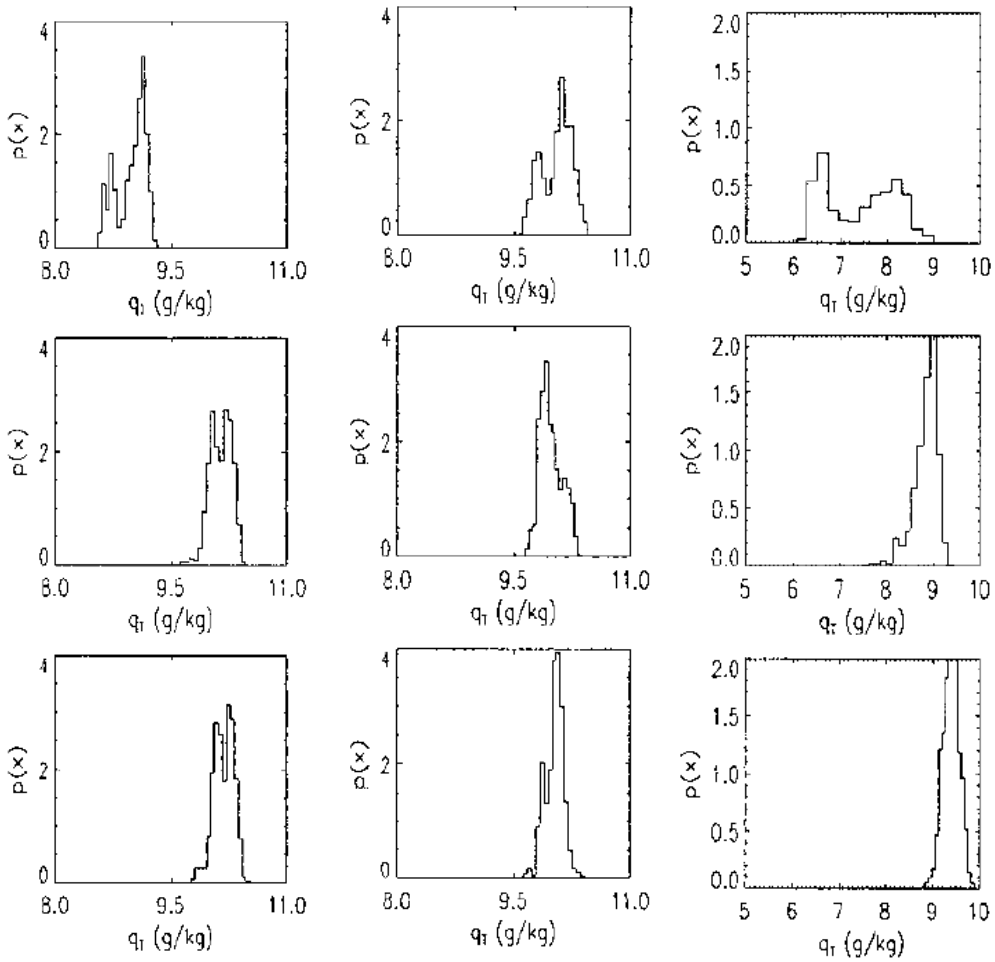

Figure 5: Reproduction total water PDFs from the aircraft observational study of Wood and Field (2000). Refer to the original article for details.

PDFs that included positive or negative skewness were able to give an improved fit the data. Price (2001) used tethered balloon data of PBL humidity collected during a three year period, finding that roughly half of the data could be classified as symmetrical or skewed unimodal. A further 25% of the data could be regarded as multi-modal.

Although many of the above studies reported a significant frequency of occurrence of distributions classed as bi- or multi-modal, these distributions often possessed a single principle distribution peak, as in the example given by Price (2001), and thus a unimodal distribution could still offer a reasonable approximation to these cases. This also applies to the flight data examples shown in Heymsfield and McFarquhar (1996) taken in ice clouds. Additionally, the bimodal and multi-modal distributions may be exaggerated in both flight and balloon data due to under-sampling. Satellite data on the other hand can give a more global view at relatively high spatial resolutions. Two such studies have been reported by Wielicki and Parker (1994) and Barker et al. (1996) who used Landsat data at a resolution of 28.5 metres to examine liquid water path in a large variety of cloud cover situations. They reported unimodal distributions in nearly or totally overcast scenes, and exponential-type distributions in scenes of low cloud fraction, as expected since in these cases only the tail of the q_t distribution is detected. Note that the analysis of LWP is likely to lead to much smoother (and thus more unimodal) PDFs due to the vertical integration.

In summary, it appears that in the observational data available conducted over a wide variety of cloud conditions (although rarely in ice-clouds), approximate uni-modality was fairly widespread, and that a flexible unimodal function can offer a reasonable approximation to the observed variability of total water. That said, a significant

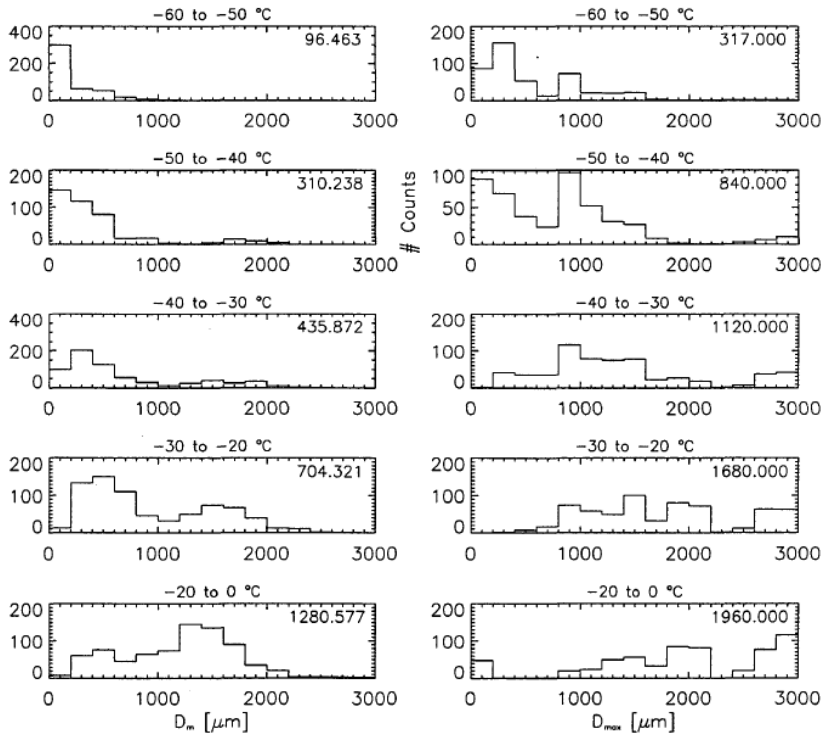

Figure 6: Reproduction of ice water content PDFs from the aircraft observational study of Heymsfield and McFarquhar (1996). Refer to the original article for details.

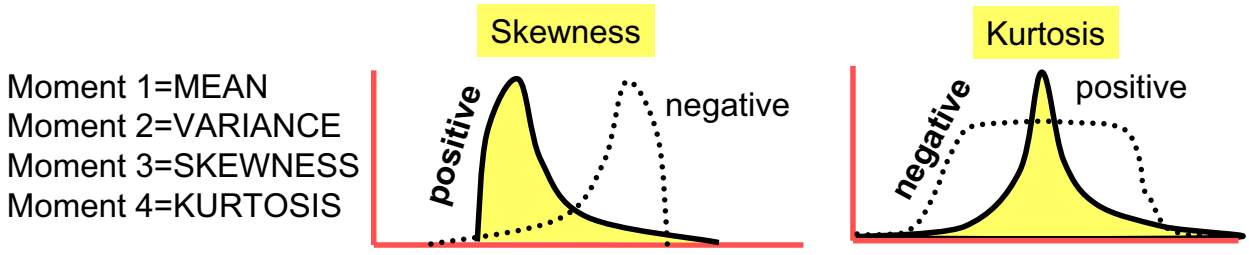

Figure 7: Schematic illustrating the 3rd and 4th moments; skewness and kurtosis.

minority of cases are very likely to be better modelled using a bimodal distribution like those advocated by Lewellen and Yoh (1993) and Golaz et al. (2002).

4.2 Setting the PDF moments

The second task of statistical schemes is to define the higher order moments of the distribution. If the distribution is simple, such as the uniform distribution, then it is defined by a small number of parameters. In the case of the uniform distribution, one could specify the lower or upper bounds of the distribution; two parameters are required. Equivalently, one could give the first two distribution moments: namely the mean and the variance. Likewise, more complicated PDFs that require 3 parameters can be uniquely defined using the first three moments: mean, variance and skewness; four-parameter distributions need the fourth moment of kurtosis (describing the PDF 'flatness', see schematic in Fig. 7), and so on.

It is clear to see why the accurate specification of the moments is important. The schematic of Fig. 8 shows

that, even if the distribution mean is correct, diagnosing a variance that is too small (i.e. the distribution is too narrow) will lead to the incorrect prediction of clear sky conditions.

Some schemes diagnostically fix the higher order moments of the distribution, such as the variance. However, it is clear that this is not an ideal approach, since by having a fixed distribution width (for example), the PDF (and thus cloud properties) are not able to respond to local dynamical conditions. The fixed width (and higher order moments) are then equivalent to the specification of the critical relative humidity at which cloud is assumed to form in the *RH* schemes.

To illustrate this with a specific example, let us consider the uniform distribution adopted by LeTreut and Li (1991). The PDF for a typical partially cloudy grid box is shown in Fig. 9. Considering the humidity, it is assumed that no supersaturation exists as is usual, and thus in the cloudy portion, $q_v = q_s$. Thus the grid-mean humidity can be written as:

$$\overline{q_v} = Cq_s + (1-C)q_e \tag{7}$$

where q_e is the humidity in the 'environment' of the cloud; the cloud-free part of the gridbox. From the uniform distribution shape, it is possible to define q_e in terms of a critical *RH* for cloud formation RH_{crit}:

$$q_e = q_s(1-(1-C)(1-RH_{crit})). \tag{8}$$

The definition of *RH* is $\overline{q_v}/q_s$, which substituting the definitions above gives

$$RH = 1-(1-RH_{crit})(1-C)^2, \tag{9}$$

which can be rearranged to give

$$C = 1-\sqrt{\frac{1-RH}{1-RH_{crit}}}. \tag{10}$$

This is recognised to be the relative humidity scheme used by Sundqvist et al. (1989). Thus it is seen that a so-called statistical scheme with fixed moments can be reduced to a *RH* scheme, or likewise that *RH* schemes do not need to rely on ad-hoc relationships, but can be derived consistently with an assumed underlying PDF of total water. This point was fully appreciated by Smith (1990), whose work actually provides the *RH*-formulation associated with the triangular distribution in its appendix.

In summary, it is important to stress that there is not a clear distinction between the so-called '*RH* schemes' and statistical schemes. If a time-invariant variance is used in a statistical scheme, it can be reduced to a *RH*-type formulation and we have seen how the *RH* scheme of Sundqvist et al. (1989) can be derived by assuming a uniform distribution for total water, and likewise that the Smith (1990) scheme also reduces to an equivalent *RH* formulation.

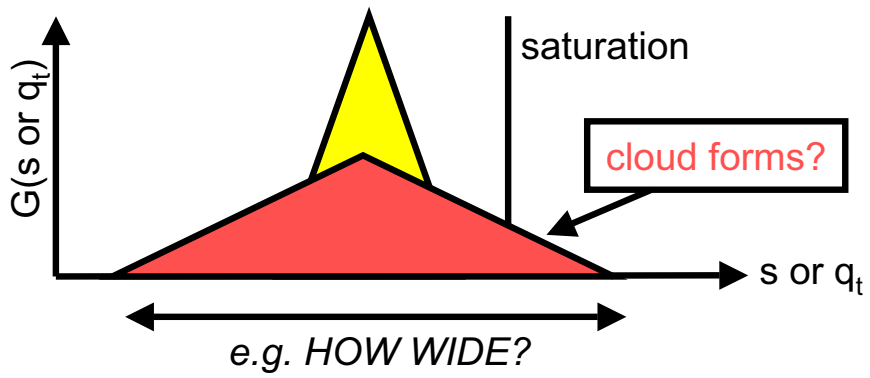

Figure 8: Even if the mean total water is correct, if the incorrect distribution width is diagnosed, for example the narrow yellow distribution, then clear sky conditions will prevail when in fact partial cloud cover exists (pink triangle).

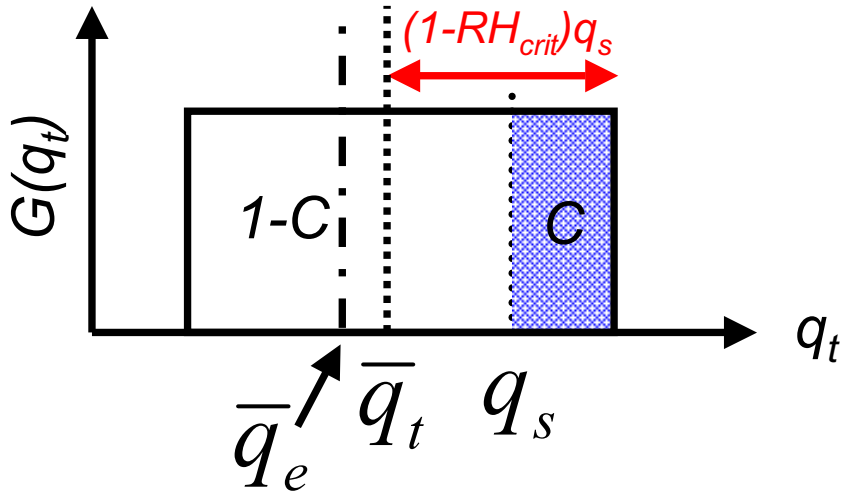

Figure 9: Graphical aid to the derivation of the cloud cover as a function of the RH when the total water is assumed to be uniformly distributed. If cloud begins to form at RH_{crit} then the width of the distribution is $2q_s(1-RH_{crit})$. See text for details.

5 Accounting for temperature variability

In this lecture fluctuations of temperature are ignored for simplicity. However, since water vapor perturbations can be correlated with temperature perturbations, which alter the local saturation vapor pressure, it may also be necessary to consider temperature variability. To this end, it has been useful to form a variable, s, defined as[4]

$$s = a_l(q'_t - \alpha_l T'_l) \tag{11}$$

where q'_t is the fluctuation of the total water mixing ratio, q_t, equal to the sum of the vapor (q_v), cloud ice (q_i) and liquid cloud water (q_l) mixing ratios, and T'_l is the liquid water temperature fluctuation ($T - \frac{L}{C_p}q_l$), an analogue to moist static energy. The fluctuations are defined about the mean thermodynamic state, $\overline{T_l}$, and the constants are defined as $\alpha_l = \frac{\partial q_s}{\partial T}(\overline{T_l})$ and $a_l = [1 + \frac{L}{c_p}\alpha_l]^{-1}$, where q_s is the saturation vapor mixing ratio, L is the latent heat of vaporization and c_p is the specific heat of dry air. Physically, s describes the distance between the thermodynamic state to the linearized saturation vapor mixing ratio curve, as illustrated in Fig. 10.

Defining $s_s = a_l(q_s - \overline{q_t})$ the cloud condensate mass q_c ($= q_l + q_i$) is given by $q_c = s - s_s$, providing $s > s_s$. Assuming that any supersaturation efficiently condenses to cloud, it is possible to express the cloud fraction C as

$$C = \int_{s_s}^{\infty} G(s)ds \tag{12}$$

where $G(s)$ is the PDF of s.

The variance of s, and therefore the associated liquid water and cloud cover, depends on the correlation between T_l and q_t perturbations in addition to their respective magnitudes:

$$\sigma^2(s) = a_l^2(\overline{q_t'^2} + \alpha_l \overline{T_l'^2} - 2\alpha_l \overline{q'_t T'_l}). \tag{13}$$

This aspect was disregarded by many previous statistical schemes, which were formulated in terms of s, but simply set the variance to a fixed or arbitrary value. In such schemes it is not known whether cloud is a result of temperature perturbations, water perturbations, or a combination of the two. For example, the scheme of Smith

[4]Once again, the commonly used notation is repeated here, but this variable is not to be confused with the more common use for s, which is the dry static energy

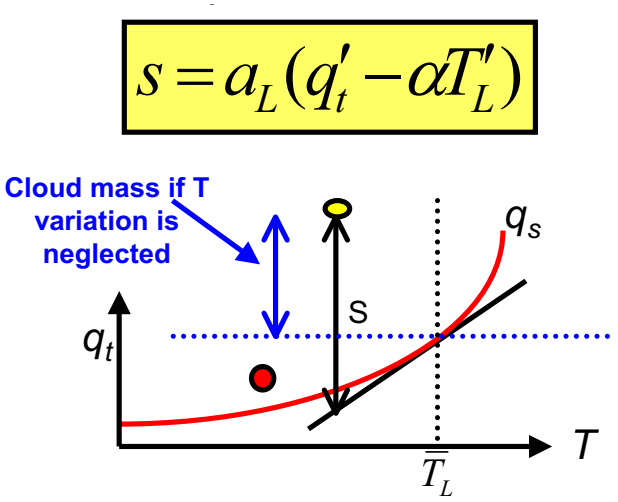

Figure 10: Schematic showing the definition of s, in terms of q_t. See text for details.

(1990) appears to take temperature perturbations into account since it is written in terms of the *s* variable, and is often cited as doing so, but in fact the use of a fixed distribution width means that the scheme can be equivalently written as a function of relative humidity. In other words, all of the subgrid thermodynamic variability leading to clouds could be solely due to humidity fluctuations, or equally due to temperature fluctuations. As stated earlier, the author of the Smith (1990) scheme was fully aware of this fact and provided the equivalent relative humidity formulation in the appendix.

The *s* variable formulation is convenient if one is able to explicitly specify the temperature and humidity fluctuations and their cross correlations and some parametrizations such as Ricard and Royer (1993) have calculated temperature perturbations separately that result from turbulence, since the turbulence scheme can provide the various correlations of $\overline{q_t'^2}, \overline{T_l'^2}$ and $\overline{q_t' T_l'}$ separately. The schemes of Lappen and Randall (2001) and Golaz et al. (2002) are further examples.

The question still needs to be asked whether it is necessary to account for temperature fluctuations in cloud schemes, or if accounting for total water fluctuations will allow one to specify the basic cloud properties such as cloud cover to a reasonable level of accuracy, given the uncertainty in other aspects of the schemes such as the ice microphysics. Temperature fluctuations are likely to be smaller in magnitude than total water fluctuations, especially in the tropics where gravity waves remove buoyancy fluctuations on fast timescales (Bretherton and Smolarkiewicz, 1989). The study of Price and Wood (2002) indicates that temperature fluctuations, while significant, are less important than humidity fluctuations, even in the lower troposphere in midlatitudes.

Tompkins (2003) made further investigations using aircraft data from various field campaigns associated with the ARM program. An example of the relative error made when temperature and humidity errors are neglected is reproduced in Fig. 11. It clearly shows that humidity fluctuations have a larger influence on cloud cover error than temperature, even for the dataset studies here which consisted mostly of boundary layer clouds below 4km. The reader is referred to Tompkins (2003) for further details. This indicates that the first order task of a cloud scheme is to represent the variability in total water.

6 Joint PDFs of temperature, total water and velocity

Even if humidity (total water) variability is the prime consideration for cloud schemes, the previous section indicated that temperature has a non-negligible influence. It was pointed out that knowing the temperature and humidity fluctuations separately were not adequate; the cross correlation $\overline{T_l' q_t'}$ must also be known. One

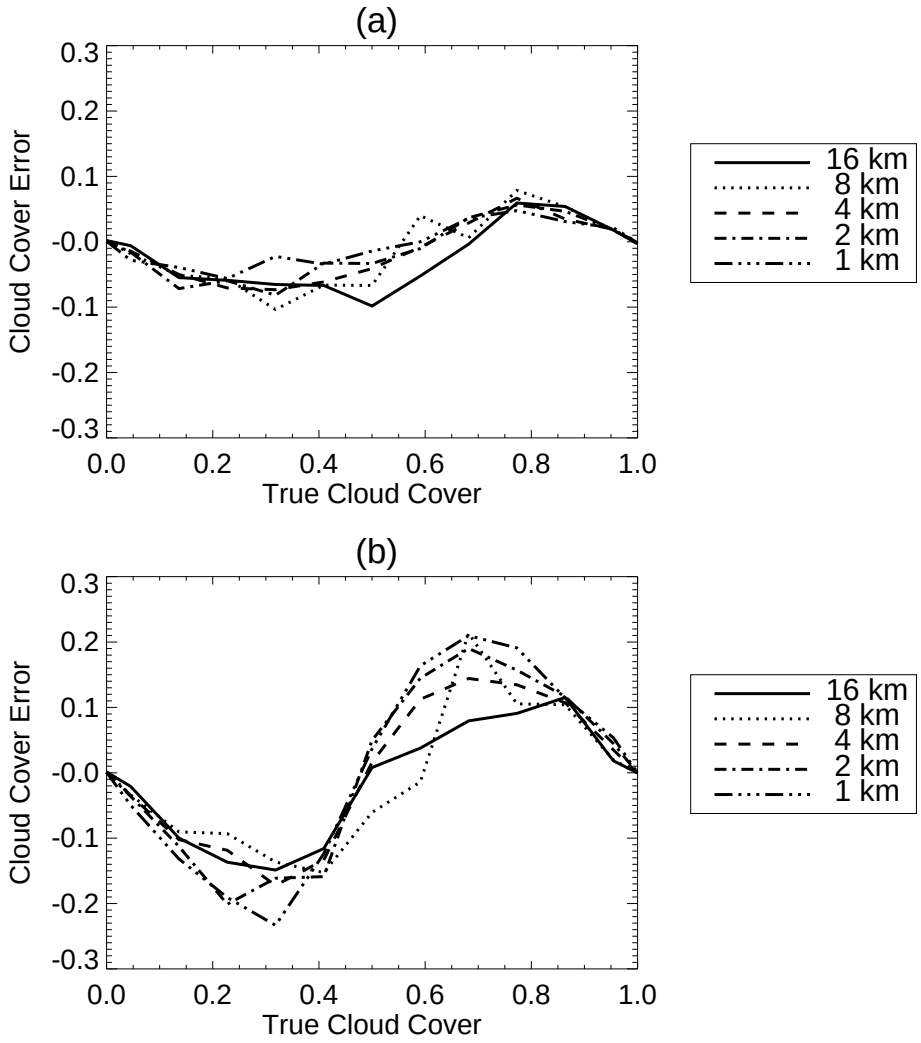

Figure 11: Cloud cover error as function of true cover for leg lengths ranging from 1 to 16 km when (a) temperature and (b) humidity fluctuations are ignored in turn. From Tompkins (2003).

methodology would be to introduce a scheme using joint-PDFs of these variables. In fact the Golaz et al. (2002) introduces a joint-PDF that also incorporates vertical velocity.

The complication that exists when specifying cross-correlations of the thermodynamic variables is that the correlation depends on the horizontal scale of motion considered most relevant for the clouds within the grid-box, which would tend to be the scale of the motion on the scale of the grid-cell. Phelps and Pond (1971); Donelan and Miyake (1973); Paluch and Lenschow (1991); Mahrt (1991) and Williams et al. (1996) all found that temperature and humidity are positively correlated over the small length scales but the correlation becomes negative for longer spatial scales, with the cross-over occurring on a scale between a few hundred metres and 2km. Tompkins (2003) found this cross-over to be at a spatial scale of about 500m averaged over all the flight legs studied.

As discussed by Mahrt (1991) and others, the positive correlation is expected in small scale buoyant updraughts, while a negative correlation would be associated with mesoscale motions. Thus if the temperature and humidity cross-correlations were to be provided by a turbulence scheme that considers the small-scale turbulent eddies, this will not be relevant for the cloud cover determining processes occurring with-in the grid-cell. Instead, Tompkins (2003) found that in the cases where the cross correlation was the strongest, a good fit to the data could be achieved by assuming either dry or moist large-scale adiabatic ascent, as shown in figure 12.

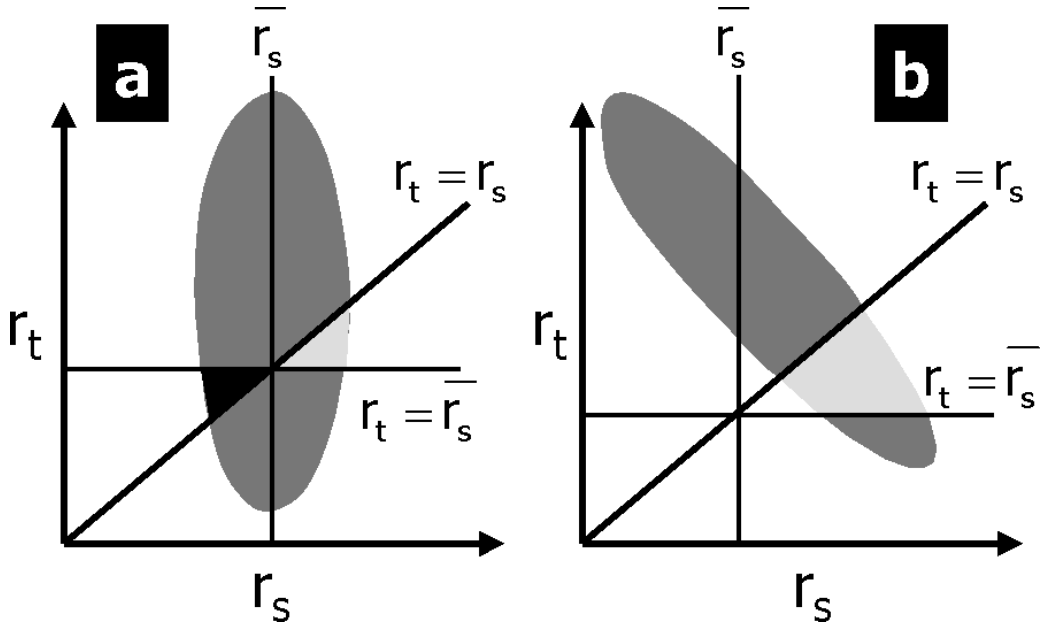

Figure 12: Schematic to illustrate why cloud cover errors are smaller when $\overline{T'r'_t}$ is small (r_t is the total water mixing ratio). The ellipse in each case represents the envelope of phase space of $[r_t, r_{sat}]$ for a particular aircraft leg. A zero skewness of both r_t and r_{sat} is assumed, such that the data points are symmetrically distributed around the mid point of the ellipse. From Tompkins (2003).

These observational results were confirmed in a carefully analysed set of large-eddy simulations conducted by de Roode et al. (2004). As the simulations progressed, starting from initially quasi-homogeneous initial conditions, de Roode et al. (2004) found that the dominant scale of the cloud organisation and associated temperature and humidity fluctuations grew from the small eddy scale to the mesoscale, with the scale restricted only by the domain size. Moreover, they confirmed that on the meso-scale the temperature and humidity fluctuations were of opposite sign with magnitudes such that the variability of the virtual potential temperature θ_v was limited. Thus it appears that mesoscale motions act to remove buoyancy fluctuations occurring due to the mesoscale organisation of the water vapour and cloud field, and it is these correlations that should be included into a cloud scheme rather than the fluctuations on the scale of turbulent eddies. The assumption that temperature fluctuations negate the buoyancy perturbations associated with mesoscale variability of humidity and cloud water was therefore used as the central axiom in the parametrization of subgrid temperature variability in Tompkins (2008).

Another practical aspect pointed out by Tompkins (2003) is that, if the sole purpose of the parametrization of subgrid-scale variability is to derive cloud cover, then if the cross-correlation term $\overline{T'_l q'_t}$ is small, and temperature and humidity perturbations are independent, then to a good approximation *the temperature perturbations can be neglected altogether*. This was due to two reasons. Firstly, one should consider that the source of (correlated) temperature and humidity fluctuations are atmospheric motions, whether small or meso-scale, which are dissipated by gravity wave dispersion and mixing, respectively. These dissipation processes operate on different timescales, and thus cases where the cross-correlation $\overline{T'_l q'_t}$ is small tend to be those in which temperature (equivalently saturation mixing ratio) fluctuations are also expected to be small, which was confirmed to be the case in the observations of Tompkins (2003). The second reason is that if $\overline{T'_l q'_t}$ is close to zero, the errors in diagnosing cloud cover from neglecting temperature variability tend to cancel out, which was illustrated in the schematic of Tompkins (2003) and reproduced here in Fig. 13. The effectiveness of this cancellation depends on the magnitude of the distribution higher order moments however, with less cancellation occurring with strongly skewed distributions. That said, knowledge of temperature fluctuations may be required/useful for other reasons. While small-scale temperature variability may have limited impact on radiative heating rates, it may be useful for convective triggering decisions, or indeed in stochastic physics treatments (extending the

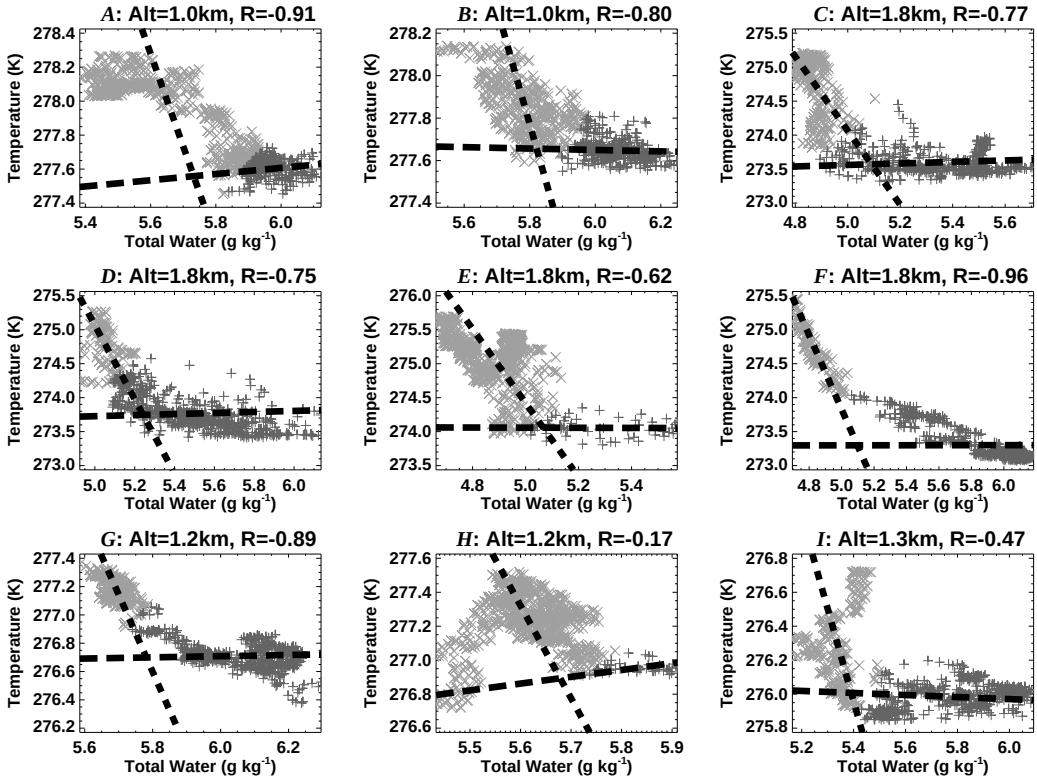

Figure 13: Scatter-plot of temperature versus total water for nine selected 16 km legs from a flight on 29th April, 1998 (see Tompkins (2003) for details on the data). Clear sky points are marked by a light X, while dark crosses (+) represent cloudy points. The dotted and long dashed lines represent the predicted gradients of the T, r_t relationship for the clear and cloud points, respectively (see text for details of calculation). Note that only the slopes of these lines is relevant; the lateral position relative to the data points has no physical significance. The title gives the altitude of each leg, and the simple linear correlation coefficient for all the points. These nine cases were selected for the high quality of the fit. From Tompkins (2003).

approach of Tompkins and Berner, 2008, for example).

7 Diagnostic versus Prognostic schemes

At this point we pause to consider the merits or otherwise of prognostic versus diagnostic cloud schemes, and by this, we mean whether or not to include a prognostic equation for the central parameters of the scheme in question. In the case of the statistical schemes this is likely (but not necessarily) to imply a memory (a prognostic equation) for the higher order moments such as variance, where as in the Tiedtke Scheme approach outlined below the prognostic variable is the cloud cover itself.

Irrespective of the variable in question, the underlying question is always whether *the variable has a fast equilibrating timescale relative to the timestep of the model*. Let us take the case of turbulence (Lenderink and Siebesma, 2000). The prognostic equation for variance is:

$$\frac{d\sigma^2(q_t)}{dt} = -2\overline{w'q_t'}\frac{dq_t}{dz} - \frac{\sigma^2(q_t)}{\tau} \tag{14}$$

The two terms on the right represent the creation of variance due to a turbulent flux of humidity occurring in the presence of a humidity gradient, and a dissipation term modelled by a Newtonian relaxation back to isotropy with a timescale of τ. This equation is highly simplified by the neglect of both turbulent and large-scale flow

transport of variance, and also the horizontal gradient terms, but it serves its illustrative purpose.

It would be possible to introduce a prognostic predictive equation for total water variance along these lines. However, if the dissipative timescale τ is very short compared to the model timestep, then a very good approximation could be obtained by assuming $\frac{d\sigma^2(q_t)}{dt} = 0$, giving

$$\sigma^2(q_t) = -2\tau\overline{w'q'_t}\frac{dq_t}{dz}. \tag{15}$$

A diagnostic approach has the advantage that it simplifies implementation, and saves computational cost and memory. The simplification does not imply that the local cloud properties are independent of the local dynamics; a scheme based on eqn. 15 can not be reduced to a *RH* scheme, since the variance in each gridbox is related to the local turbulent flux. Note also that now, with such an approach, one can sensibly include the contribution of temperature fluctuations due to turbulence, as done by Ricard and Royer (1993).

For examples of this kind of approach, examine the diagnostic schemes in the literature that are described by Bougeault (1982); Ricard and Royer (1993); Bechtold et al. (1995); Lohmann et al. (1999); Chaboureau and Bechtold (2002). These schemes mostly restrict their concern diagnostic relationships for variance to the influence of turbulence. For example, above the boundary layer, Lohmann et al. (1999) imposed a fixed width distribution to compensate for the lack of consideration of other processes.

It is thus apparent that for generalized cloud situations, that include the evolution of clouds such as large-scale cirrus, which may evolve over many hours or even days, it will normally be necessary to resort to implementing a prognostic approach.

8 A prognostic statistical scheme

To the author's best knowledge, the first attempt to implement a fully prognostic statistical scheme into a GCM was made by Tompkins (2002). This modelled the total water fluctuations using a Beta distribution,

$$G(t) = \frac{1}{B(p,q)}\frac{(t-a)^{p-1}(b-t)^{q-1}}{(b-a)^{p+q-1}} \qquad (a \le t \le b) \tag{16}$$

where a and b are the distribution limits and p and q are shape parameters (Fig. 14)[5] and the symbol B represents the Beta function, and can be defined in terms of the Gamma function, Γ, as follows:

$$B(p,q) = \frac{\Gamma(p)\Gamma(q)}{\Gamma(p+q)}. \tag{17}$$

The skewness (ς) of the distribution is related to the difference between the two shapes parameters p and q,

$$\varsigma = \frac{2(q-p)}{p+q+2}\sqrt{\frac{p+q+1}{pq}}, \tag{18}$$

and thus if $p = q$ the distribution is symmetrical, but also both positive and negatively skewed distributions are possible. As p and q tend to infinity the curve approaches the Normal distribution. The standard deviation of the distribution is given by

$$\sigma(t) = \frac{b-a}{p+q}\sqrt{\frac{pq}{p+q+1}} \tag{19}$$

Although this distribution is a 4-parameter function, a diagnostic closure such as imposing $p+q$ =constant can reduce it to a three parameter distribution (regrettably Tompkins instead used the much less elegant p=constant

[5] the original notation is repeated, but please note that the shape parameter q is not to be confused with mixing ratio, q_v.

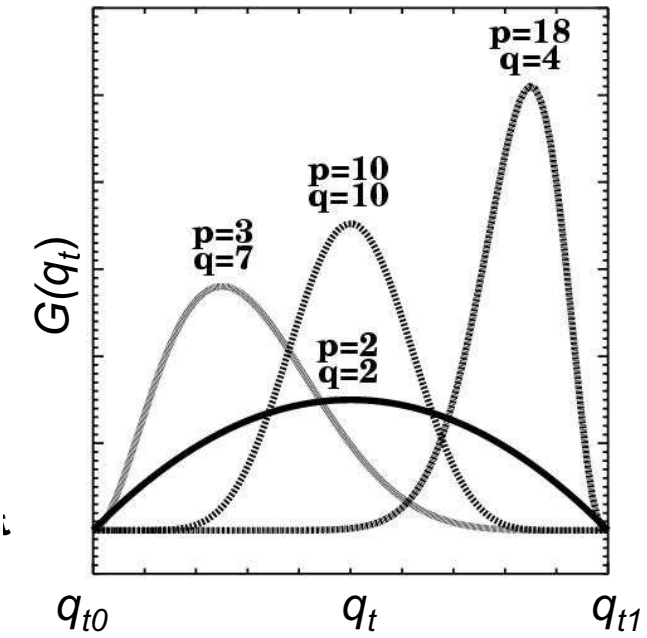

Figure 14: Examples of the Beta distribution for various shape parameters. From Tompkins (2002). The distribution minimum and maximum are referred to as a and b in the main text.

closure, which unnecessarily restricted to distribution to positive skewness regimes). This avoids the necessity of considering the fourth-order kurtosis budget and the distribution can be specified uniquely by the mean, variance and skewness of total water. This is discussed further in the following section.

Tompkins (2002) attempted to introduce two additional prognostic equations to predict the evolution of the PDF shape. Once the distribution shape is known, (i.e. distribution limits a and b and the shape parameters p and q) the cloud cover can be obtained from

$$C = 1 - I_{\frac{q_s - a}{b-a}}(p,q), \tag{20}$$

where I_x is the incomplete Beta function ratio defined as

$$I_x(p,q) = \frac{1}{B(p,q)} \int_0^x t^{p-1}(1-t)^{q-1} dt, \tag{21}$$

subject to the limits $I_0(p,q) = 0$ and $I_1(p,q) = 1$.

Tompkins (2002) then attempted to parametrize the sources and sinks of variance and skewness separately from physical processes such as convection, turbulence, microphysics and so on. However, there is one complication that requires consideration, and is summarized by the following equation for cloud water q_c:

$$\bar{q_c} = (b-a)\frac{p}{p+q}(1 - I_{\frac{(q_s-a)}{(b-a)}}(p+1,q)) + (a-q_s)(1 - I_{\frac{(q_s-a)}{(b-a)}}(p,q)), \tag{22}$$

This is simply eqn. 6, with the Beta distribution substituted for $G(q_t)$. This tells us that if the distribution moments are known, then the cloud water is uniquely defined. Why is this a cause for concern? The reason is that *most cloud schemes already implement a separate prognostic equation for cloud liquid/ice water*. In other words, in partially cloudy conditions, if distribution moments *and* the cloud liquid water are given from the respective prognostic equations, then the problem is potentially over-specified. To clarify this we can re-examine the simple 2-parameter triangular distribution in Fig. 15. The figure shows that the 2-parameter distribution can be uniquely defined by giving either the mean and variance, or the mass mixing ratios of vapour and cloud water separately.

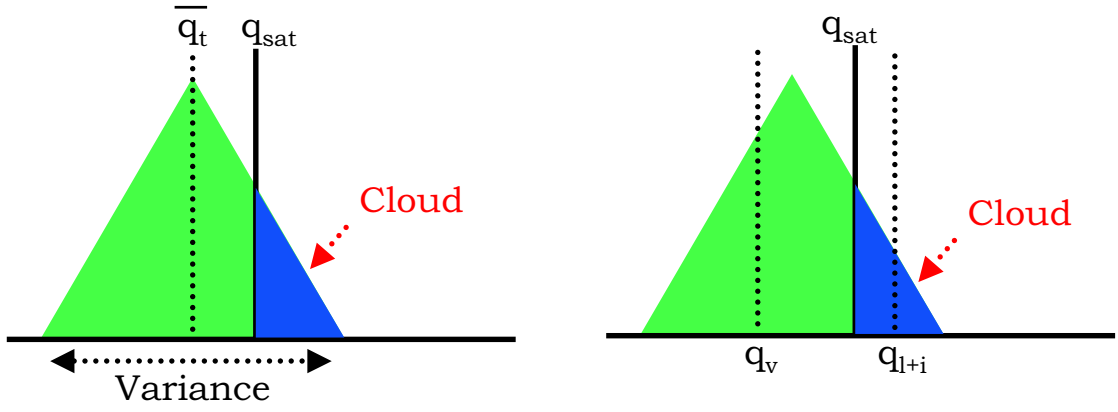

Figure 15: Schematic of the two ways of specifying the triangular distribution. Left Panel: The distribution mean and variance is given. Right Panel: The mean vapour and cloud water (ice+liquid) are given. In both cases the distribution is uniquely specified and the cloud cover can be diagnosed.

Thus a decision must be reached concerning the prognostic equation set to be used. The first option is to use water vapour and cloud water separately to implicitly derive the variance (right panel of Fig. 15). The advantage of this approach is that one does not need to explicitly derive complex variance source/sink terms, such as the impact of microphysics on variance. If, over a timestep, the microphysics reduces the cloud water (for example by autoconversion to snow, or by settling out of the gridbox) then this implicitly renders a narrowing of the distribution. However, it is clear that by working on the grid-mean cloud water the contribution to the variance budget by nonlinear processes will be incorrect (as will the contribution to the cloud water budget itself incidentally). Additionally it is much easier to ensure conservation of cloud water (presuming the numerics employed are designed to ensure conservation of prognostic quantities). The disadvantage is that *the information is only available in partially cloudy conditions*. In clear sky conditions one only knows the distribution mean, since $q_c = 0$ identically (see schematic of Fig. 16). Likewise in overcast conditions, where $q_v = q_s$. In these situations, the loss of information requires supplementary ad-hoc assumptions to be made, to close the system. For example, one could resort to assuming a fixed distribution width in clear-sky conditions, thus returning to cloud formation at a specified (RH_{crit}). We will see below that this issue arises once again in the Tiedtke (1993) scheme, which resorts to such a solution.

The second approach is to abandon the separate cloud water prognostic variable in favour of a prognostic variance equation. This has the advantage that the distribution is *always* known, even in clear sky or overcast conditions. The disadvantage is that all sources and sinks must now be parametrized in terms of variance sources and sinks. For turbulence (Deardorff, 1974), and perhaps convective sources and sinks (Lenderink and Siebesma, 2000; Klein et al., 2005), this is relatively straight-forward. However, for the microphysical processes the problem quickly becomes complicated. For a microphysics conversion term M such as simple autoconversion terms (the rate of conversion from liquid to rain), it is possible to derive the sink of variance[6]

$$\frac{d\sigma^2(q_t)}{dt} = \overline{M' q_t'} = \int M'(q_t) q_t' G(q_t) dq_t, \tag{23}$$

which analytically tractable for simple forms of A and $G(q_t)$. Nevertheless, we can imagine more complicated scenarios, such as ice settling handled by a semi-Lagrangian advection scheme, allowing settling from any

[6]Care that must be taken with regard to the numerics with long timesteps. Since autoconversion terms tend to be nonlinear they usually reduce the variance. Even if this equation is integrated implicitly for stability, the limit for long timesteps will be zero, which is unrealistic for partially cloudy conditions since the precipitation process does not affect the clear sky part of the domain. Thus instead one should integrate this term implicitly for the cloudy portion [cld] of the gridcell and then combine the result with the clear sky [clr] variance thus: $\overline{\sigma^2(q_t)} = C(q_s^2 + \sigma^2(q_t)[cld]) + (1-C)(q_v^2[clr] + \sigma^2(q_t)[clr]) - \overline{q_t^2}$. The issue of numerics is revisited later in this document.

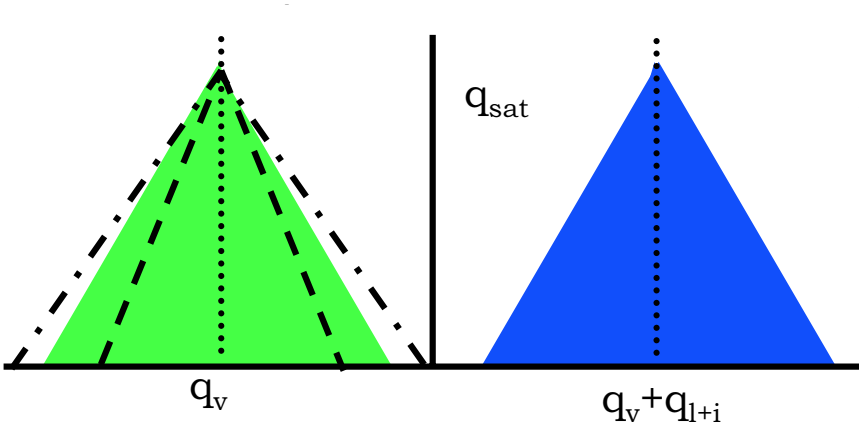

Figure 16: Schematic of the problem that arises if distribution width is derived from separate prognostic equations for vapour and cloud water. The curve is not uniquely defined for overcast (blue PDF) or clear sky (green PDF) conditions. For example, for the clear-sky case, there are any number of possible variances (width) of the distribution that give the correct mean water vapour and zero cloud water. Two examples are marked: a wider distribution (dot-dashed) or narrower (dotted).

particular gridbox to other all levels below it. Trying to parametrize this equivalently in terms of variance sources and sinks is difficult. Moreover, by abandoning the prognostic equation for ice, any inaccuracies in the handling of such a process via a variance equation are likely to manifest themselves in a compromising of the cloud mass conservation.

Tompkins (2002) tried to provide a solution for this dilemma by implementing a hybrid scheme. In partially cloudy conditions variance is derived directly from the cloud water and vapour prognostic equations. In clear sky and overcast conditions, the variance is prognosed using a subset of source and sinks terms, including turbulence, dissipation, and a highly simplified sink term due to microphysics, which is necessary in overcast conditions. The reader is referred to Tompkins (2002) for details of these source and sinks terms, although it should be noted that some of these, in particular the skewness budget terms from microphysics and deep convection, have been justifiably criticized by Klein et al. (2005) for their ad hoc nature. Nevertheless, the inclusion of even a reduced set of variance sources/sinks, especially from turbulence, is able to reproduce the observations of turbulence increasing or decreasing variance according the mean humidity gradients, and coincidentally creating cloud or breaking-up an overcast cloud deck (Fig. 17).

8.1 Future developments of the Tompkins scheme

The Tompkins (2002) scheme has a number of shortcomings, not least the hybrid approach of using a contrasting prognostic equation sets depending on the meteorological conditions, and the ad-hoc way in which some of the source/sink terms are derived. Currently there is no scheme in existence to the author's knowledge that implements a fully prognostic statistical scheme with sources and sinks of the variance, skewness and other necessary moments derived for each atmospheric process such as convection and complex cloud microphysics fully from first principles. This section highlights some areas in which progress can be made.

8.1.1 The prognostic equation set

The scheme of Tompkins used a *beta* distribution simplified to 3 defining parameters, and thus can be defined uniquely by expressing the mean, variance and skewness. The skewness of this distribution can take on any value in general, but if one restricts the distribution to the bell shaped regime (i.e. $G(r_t) \rightarrow 0$ as $q_t \rightarrow a, b$) which is demarked by $p > 1$ and $q > 1$ then the skewness is limited to be less than 2.

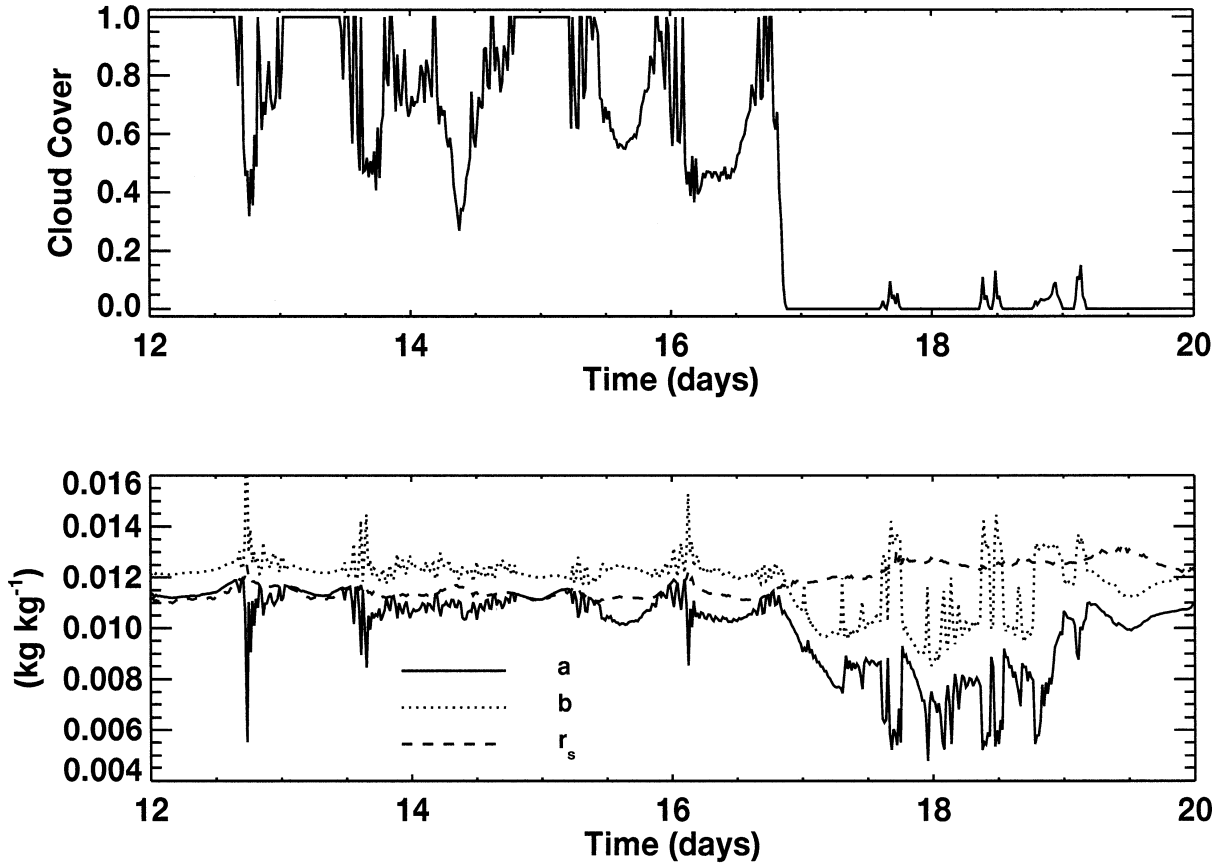

Figure 17: Figure taken from Tompkins (2002) showing evolution of the boundary layer at a gridpoint subject to stratocumulus cloud. The upper panel shows the cloud cover, while the lower shows the total water distribution minimum (a), maximum (b) in addition to q_s (marked r_s in the plot, according the notation used in that paper). In the earlier period, the scene is overcast and the whole of the PDF is moister than q_s. In this case the increase in variance from turbulence breaks up the cloud deck intermittently. In the latter period instead the gridbox is relatively dry, and turbulence instead creates small cloud coverage; representing the cloud capped thermals known as 'fair weather cumulus'.

The scheme of Tompkins used a closure which set the shape parameter p to a constant of 2. It then introduced a prognostic equation for q. One problem of this closure is that negatively skewed distributions are forbidden and the skewness is more strictly limited to $\sqrt{2}$. The equation introduced for the parameter q was rather ad hoc, with a source and a sink term. The sink was parametrized as a Newtonian relaxation back to the symmetrical PDF with $q = p = 2$. The source term was parametrized in an approximate way, relating the increase in q (and thus indirectly skewness) to the detrainment of cloud condensate at a particular level.

Jeffery (personal communication) correctly pointed out the short-comings in the Tompkins (2002) scheme and went on to suggest an alternative closure of $p+q = K$ suggesting that the quiescent solution of $p = q = 5$ gives an improved fit to aircraft observations relative to the values of $p = q = 2$ used by Tompkins (2002). As well as allowing both positive and negative skewness, this additive closure has the advantage that it can provide any value of skewness. That said, it achieves this by abandoning the Bell shape regime for the 'exponential regime' at higher skewness values, which would imply a discrete transition of the PDF and discontinuities at the PDF bounds.

Here we suggest an alternative modified closure to the Tompkins (2002) scheme. The new closure restricts the PDF form to the bell shaped regime, thus the PDF development is continuous, but with skewness permitted to take on the maximum possible range of values for this case, namely $\varsigma \in (-2,2)$. Both positive and negative

skewness values are possible with one combined shape parameter. The new closure relates the PDF shape parameters p and q as follows:

$$(p-1)(q-1) = K \tag{24}$$

where K is a constant. Thus as $q \to \infty, \varsigma \to 2$. The constant K determines the symmetrical Beta distribution eventually adopted in the absence of other processes (the 'quiescent solution'). The choice of K is based on pragmatism. Setting $K = 1$ gives the solution of $p = q = 2$ as in Tompkins (2002), but leads to complex relationship between skewness and q. If we instead select $K = 2$, this renders a quiescent solution of $p = q = 1 + \sqrt{2}$, and conveniently gives

$$pq = p + q + 1 \tag{25}$$

which allows eqn 18 to be greatly simplified. Substituting this relationship leads to the quadratic relationship between q and ς:

$$q^2 + \frac{2(\varsigma+2)}{\varsigma-2}q - 1 = 0. \tag{26}$$

For the Bell shaped regime only positive roots are physically reasonable, which leads to

$$q = \frac{(\varsigma+2) + \sqrt{2(\varsigma^2+4)}}{2-\varsigma}. \tag{27}$$

Once q is known, p is given simply from (25) as

$$p = \frac{q+1}{q-1} \tag{28}$$

Thus by implementing such pragmatic closures the conversion between the statistical moments and the PDF becomes tractable and analytical, implying a faster scheme, while the extension also permits negative skewness in addition.

8.1.2 The convective and microphysics source terms

The second criticism of the Tompkins scheme is that the derivation of the sources and sinks of the prognostic variables related specifically to deep convection and microphysics. These were derived in an indirect way, using the sources and sinks of the microphysical variables provided by these respective schemes. The translation of the humidity and cloud water tendencies into PDF moment tendencies was also approximated, due to the closure form used as described in the previous section.

Klein et al. (2005) instead showed how one could improve on this approach and directly derive the sources and sinks of variance, skewness and higher order moments from a standard mass flux convection scheme. Considering the variance, this work pictures a convective updraught detraining air with properties with a certain mean and variance of total water into an environment with contrasting properties, as depicted in Fig. 18.

For the variance budget Klein et al. (2005) described the two source terms due to a detrainment mass of D as

$$\frac{\partial \sigma^2(q_t)}{\partial t} = D(q_{td} - q_t)^2 + D(\sigma^2(q_{td}) - \sigma^2(q_t)). \tag{29}$$

The first term on the right describes the increases in variance in the environment due to the detrainment of air with different mean properties q_{td}, while the second term describes the changes due to different variance in

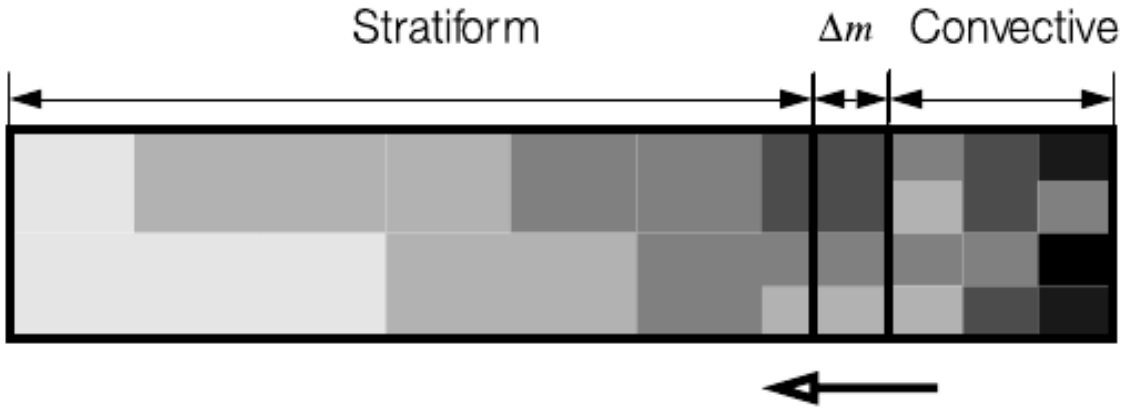

Figure 18: Schematic of a updraught detraining into the environment, with the shaded blocks illustrating total water variability of each air mass. Figure reproduced from Klein et al. (2005).

the environment. There were also two terms relating to convective entrainment and one due to compensating subsidence in the environment. The reader is referred to Klein et al. (2005) for details of the derivation.

Using a cloud resolving model to simulate deep convection and identify regions of updraught and environment air within the domain, Klein et al. (2005) were able to derive the magnitude of the sources and sinks due to these 5 terms, reproduced in Fig. 19. The figure shows that the source of variance due to each of the detrainment terms are comparable in magnitude. The concern that this raises, is that most deep convective parametrizations only provide the the updraught mean properties and not the sub-draught variability, implying that terms such as $\sigma^2(q_{td})$ are not readily available. Klein et al. (2005) examined the relationship between the mean and variance in the cloud resolving model experiments (see Fig. 20) and found that variance tended to be positively correlated with updraught mean properties, as one would expect, and suggested using this as a diagnostic closure for $\sigma^2(q_{td})$.

The problem with the diagnostic closure for $\sigma^2(q_{td})$ is that the relationship between $\sigma^2(q_{td})$ and $\overline{q_{td}}$ is very approximate, and Fig. 20 reveals considerable scatter. Moreover, for higher order moments such as skewness or kurtosis it is unlikely that any meaningful relationship with mean updraught properties holds.

An alternative approach therefore would be form a budget equation for the mass flux scheme updraught variance along the same lines as suggested for the environment. We test this closure offline using the convection scheme of ECMWF. Starting with a fixed arbitrary value of variance at cloud base related to the environmental mean humidity[7]. The formulation of Klein et al. (2005) is rewritten according to the form of Lewellen and Yoh (1993), giving the updraught variance $\overline{r'^2_u}_k$ at any vertical model level k due to an entrainment rate E as

$$\overline{q_t u'^2}_k = (1-\Delta tE)(\overline{q_{tuk-1}} + \overline{q'^2_{u\,k-1}}) + \Delta tE(\overline{q_{tk}} + \overline{q_t'^2}_k) - (\overline{q_{tk}})^2 \tag{30}$$

The results of this offline closure are shown in Fig. 21, which shows increasing variance with height within the updraught. It is highly likely that this closure significantly over-estimates the sub-plume variance, especially in the upper tropospheric deep convective cores, as this derivation only include the source term that increases variance when drier air is entrained from the environment, and thereafter remains as a distinct updraught entity without mixing with the pre-existing updraught air. The mixing of freshly entrained air parcels with updraught

[7]With a fully prognostic statistical scheme in place, the initial updraught variance could be set to the environmental value at cloud base.

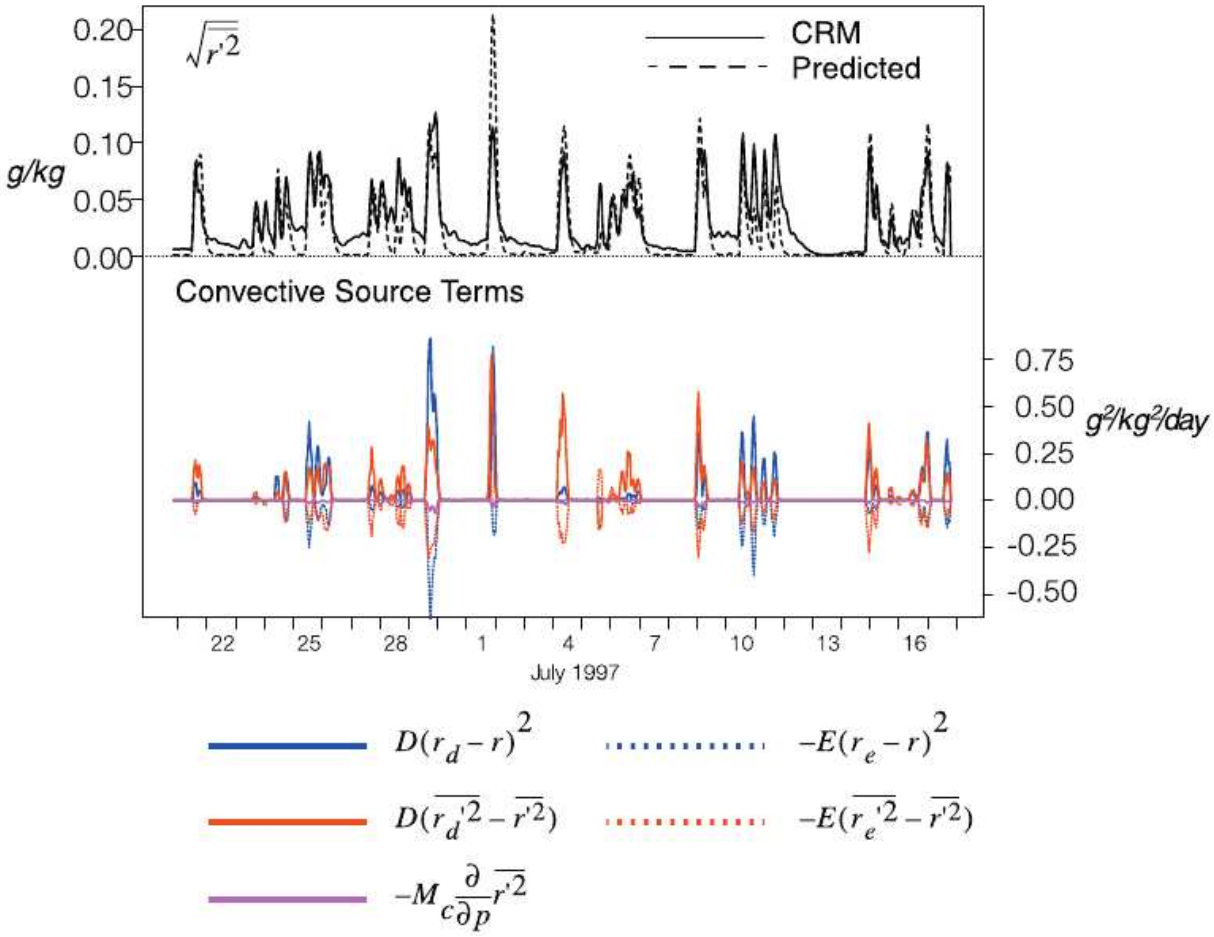

Figure 19: CRM derived q_t (r in the figure notation) standard deviation, and the derived source and sink terms. The "predicted" time evolution of the standard deviation is made using the 5 source and sink terms depicted, with the addition of a fixed-timescale Newtonian "return to isotropy" term. Figure reproduced from Klein et al. (2005)

plumes would act as a variance sink that could be represented as a Newtonian relaxation return to isotropy term. Note that this treatment of variance is at odds with the underlying bulk mass assumption of the base convection scheme, which calculates the bulk mass flux profile and cloud top using an entraining plume with homogeneous properties. In other words, a plume-based parametrization approach along the lines of Raymond and Blyth (1986) or Emanuel (1991) lends itself more readily to a self-consistent treatment of updraught variance than the bulk mass-flux methodology.

8.1.3 Microphysics

Another complication of the statistical scheme approach is the treatment of microphysics. Most existing cloud schemes carry prognostic equations for cloud variables and define the tendencies of these cloud variables due to microphysical processes directly. In a fully prognostic statistical scheme, the microphysical processes instead have to be redefined in terms of sources and sinks of the PDF moments.

As stated in Klein et al. (2005), the tendency of the total water variance due to a microphysical process $M = \frac{\partial q_x}{dt}$ that acts as a sink of total water q_t (i.e. autoconversion of liquid cloud water to rain droplets, which are not included in q_t) is related to the correlation $M'q_t'$ integrated across the grid-cell, and was given earlier in Eqn. 23.

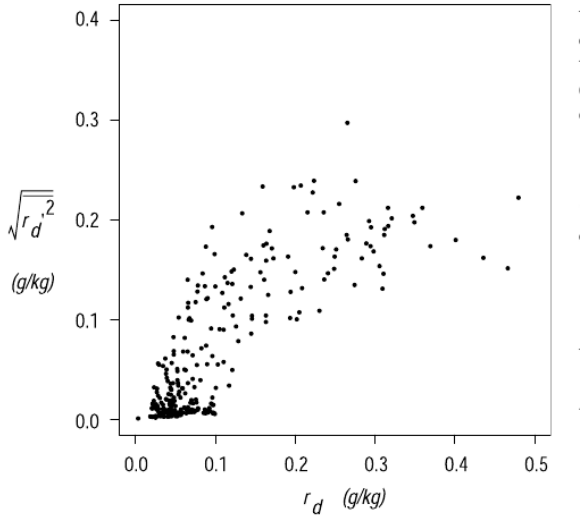

Figure 20: Relationship between $\sqrt{\sigma^2(q_{td})}$ and $\overline{q_{td}}$ from the CRM simulations of Klein et al. (2005) (note notation usage of r). Figure reproduced from Klein et al. (2005)

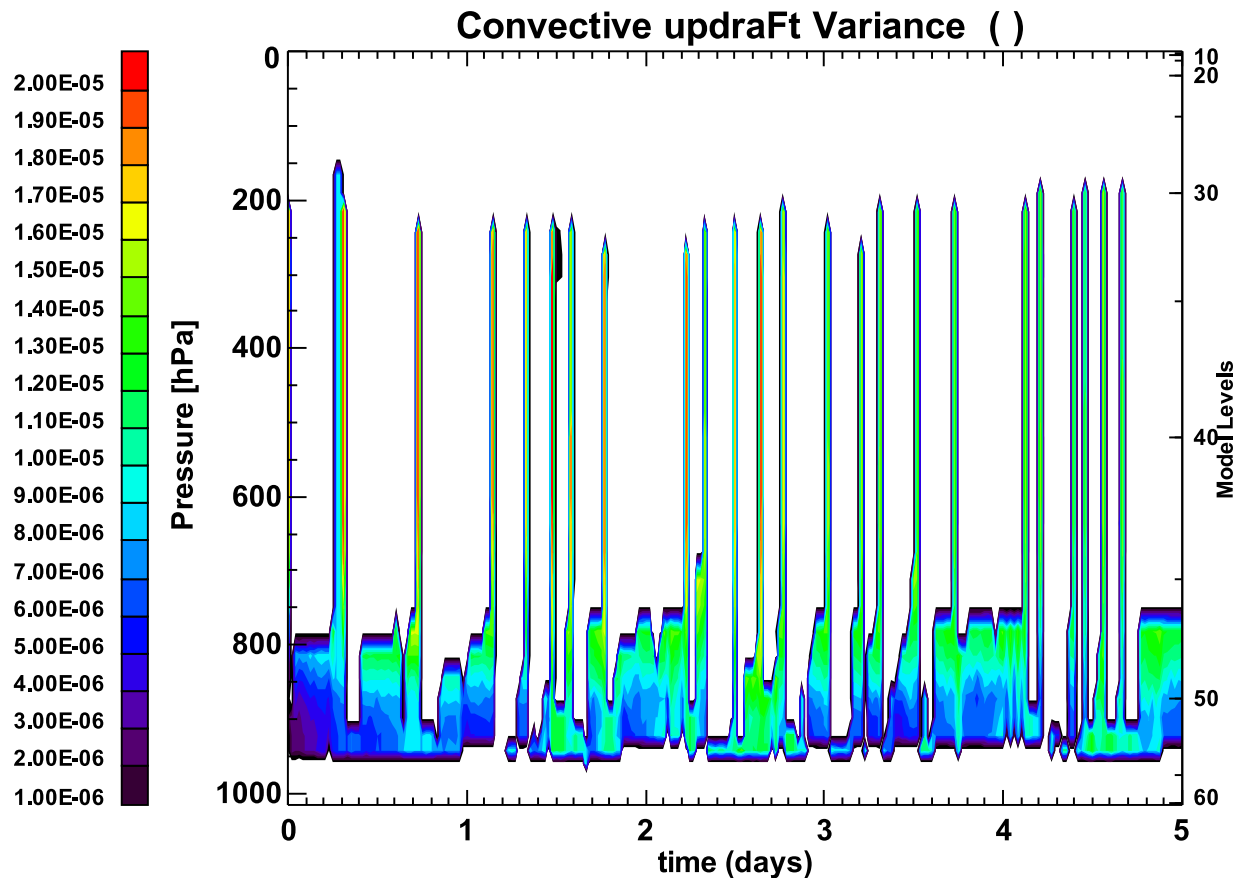

Figure 21: Offline variance calculation using the Tiedtke (1989) convective scheme

It is clear that the tractability of this integral will depend on the PDF form $G(q_t)$ and the complexity of the microphysical parametrization M in question. For example, the autoconversion form of Sundqvist et al. (1989) contains a squared exponential term in q_t making the direct solution of Eqn. 23 impossible for all but the simplest PDF forms.

One possible avenue is to approximate the microphysical sink term by only considering the effect on variance due to the reduction of the *mean* in-cloud water amount, neglecting the sub-cloud variations. This assumption is perfect if the microphysical process is linear, with accuracy of the approximation decreases with increasing nonlinearity of the process in question.

The assumption is equivalent to that of assumming a double delta function PDF for the total water, in which the variance can be defined as

$$\sigma^2(q_t) = Cq_{tc}^2 + (1-C){q_e}^2 - {q_t}^2, \tag{31}$$

where q_{tc} is the mean total water in the cloudy region of the grid-cell and q_e is given in Eqn. 7. Assuming that microphysical processes do not affect cloud fraction ($\frac{\partial C}{\partial t} = 0$) we get

$$\frac{d\sigma^2(q_t)}{dt} = C(1-C)(2q_{tc} - q_e)M \tag{32}$$

Thus, we can see that by neglecting sub-cloud variability, the variance sink due to microphysics can be derived irrespective of the complexity of the cloud water sink parametrization M, but of course, for highly nonlinear parametrizations, the approximation is quite severe.

As pointed out earlier, some ice processes, such as sedimentation, are much more complicated to represent in the statistical scheme framework. Moreover, the ice variable is further complicated by the fact that ice nucleation (homogeneous or heterogeneous) does not occur at relative humidities of 100% but at much higher thresholds (e.g. Pruppacher and Klett, 1997; Kärcher and Lohmann, 2002; Gierens, 2003). However, it is not possible to simply replace the lower integral limit q_s with this higher threshold in the statistical scheme framework of Eqns. 5 and 6, since after nucleation has occurred, ice crystal growth by deposition (often rapidly) returns the in-cloud humidity towards saturated conditions. This "hysteresis" behaviour implies that knowledge of the cloud parcel (grid-cell) history is required to represent supersaturation in the statistical scheme approach.

We therefore suggest that the statistical scheme approach lends itself best to warm rain processes, where cloud droplets can be assumed to be in suspension, and which form rapidly at a fixed threshold (and likewise evaporate below this threshold). On the other-hand, the complications of the ice phase of both non-negligible sedimentation rates of ice crystals and an hysteresis behaviour between the saturation and ice nucleation thresholds imply that cloud ice crystals could be better handled as a (or several, if the crystal size spectra is to be resolved) separate prognostic "bulk" variable(s), as is already done in many ice microphysical schemes. Thus, this hybrid approach would introduce a prognostic equation for $q_t = q_v + q_l$, with separate equations for ice, and possibly other falling bulk quantities such as snow, graupel and rain.

9 The ECMWF prognostic cloud cover scheme

The aim here is not to describe the Tiedtke (1993) scheme in detail, this is performed admirably by the work of Tiedtke (1993); Gregory et al. (2000); Jakob (2000) and the online documentation. Instead this section briefly places the Tiedtke scheme into the context of the cloud scheme family, in particular the statistical schemes. The Tiedtke scheme has many merits and has proved to be very effective in its prediction of cloud characteristics (e.g. Hogan et al., 2001).

The Tiedtke scheme chooses a different set of prognostic equations for cloud scheme, namely: water vapour, cloud water and cloud cover. We saw in the last section how the former two, vapour and cloud could be used to equivalently specify the mean and variance of total water, *in partially cloudy conditions*. The Tiedtke scheme takes this approach a step further by adding a third predicted equation, giving a memory for the cloud cover.

We also learned in the previous section that such an approach has some advantages, since it greatly simplifies some of the source and sink derivations. A good example is the link to the convection scheme. The convection scheme provides a mass of detrained cloudy air, which is then simply added directly to the respectively cloud water and cover equations, without recourse to distribution functions.

This is not to say that the Tiedtke scheme does not use assumptions concerning the underlying distributions to derive some of the sources and sinks of the prognostic equations. For example, the source of cloud water and cloud cover from a gridbox cooling is derived assuming the clear sky humidity observes a uniform distribution (note that an error in the original derivation of Tiedtke (1993) was corrected by Jakob (2000)). The assumption leads to a cloud fraction source of

$$\frac{\partial C}{\partial q_s} = -\frac{(1-C)^2}{2(q_s - q_v)} \tag{33}$$

This direct translation of PDF moment sources and sinks into consistent cloud cover and water sources and sinks is discussed in far greater detail in Wang and Wang (1999); Gregory et al. (2002); Larson (2004). In other words, in many respects *the Tiedtke (1993) approach is simply a variable transformation of the prognostic statistical scheme approach*.

Note that the Tiedtke (1993) scheme does not parametrize all sources and sinks consistently with an underlying distribution. For example, the horizontal subgrid-scale eddies act to homogenize the total water field and will reduce the width of the distribution. Thus if $\overline{q_t} < q_s$ then the cloud cover will reduce as a result, while with $\overline{q_t} > q_s$ dissipation will increase cloud cover. The Tiedtke scheme instead always reduces cloud cover, in conflict with any possible humidity distribution.

For the most part, *if* the Tiedtke scheme uses an underlying distribution assumption, it is usually that the clear sky humidity fluctuations are distributed uniformly, while the cloudy portion is homogeneous (described by a delta function). It is thus clear that the scheme is not reversible. If a gridbox is subjected to an equal magnitude cooling followed by warmed over two consecutive timesteps, and all other processes (e.g. precipitation) are neglected, there is a net creation of cloud, as illustrated in Fig. 22. The assumption that no sub-cloud variability in condensate exists, and the resulting irreversibility of the scheme, is not necessarily physically wrong; it is equivalent to the assumption that in-cloud mixing homogenizes in-cloud fluctuations on a fast time-scale compared to the model timestep. However, observations in real clouds such as the examples from Wood and Field (2000) reproduced in Fig. 5 show that the turbulent entrainment process occurring in clouds can act to introduce and increase sub-cloud variability.

One potential draw-back issue concerns self-consistency. With a pure statistical scheme approach, where the PDF moments are predicted, the cloud water and cover are constrained to be consistent with each other, since they are both derived from the same distribution. This is not true for the Tiedtke scheme, and it is not unusual for cloud water and cover to be inconsistent, with only one of the two fields non-zero for instance. On the other hand, such inconsistencies are always to be tackled in any approach. For example, with the statistical schemes, it is possible for values of variance and skewness to arise that may not be consistent with the assumed underlying distribution, or may give rise to a PDF that encompasses negative vapour amounts. These inconsistencies are simply more 'apparent' with the Tiedtke approach as they occur in bulk 'observable' quantities.

Likewise, the apparent advantages of the Tiedtke approach, such as the simpler link to the convection scheme and treatment of microphysics, exist due to the fact that all sub-cloud thermodynamic variability is neglected (only the bulk volume of cloud air is required). As we saw earlier in the discussion of microphysics (re. eqn. 32), the derivation of a prognostic statistical scheme is also vastly simplified if sub-cloud variations are neglected. In other words, statistical schemes are only more complicated as they aim to treat the higher order moments of the cloud characteristics, not due to the methodology ethos itself.

In summary, statistical approaches and the Tiedtke approach are closely related, with the former carrying the explicit properties of the thermodynamic PDFs, and the latter instead carrying the integral properties of the PDFs (cloud cover and so on), simplifying the implementation but consequently implying an associated *loss of information*. The choice of scheme approach reduces to a balance between tractability, cost and the need to

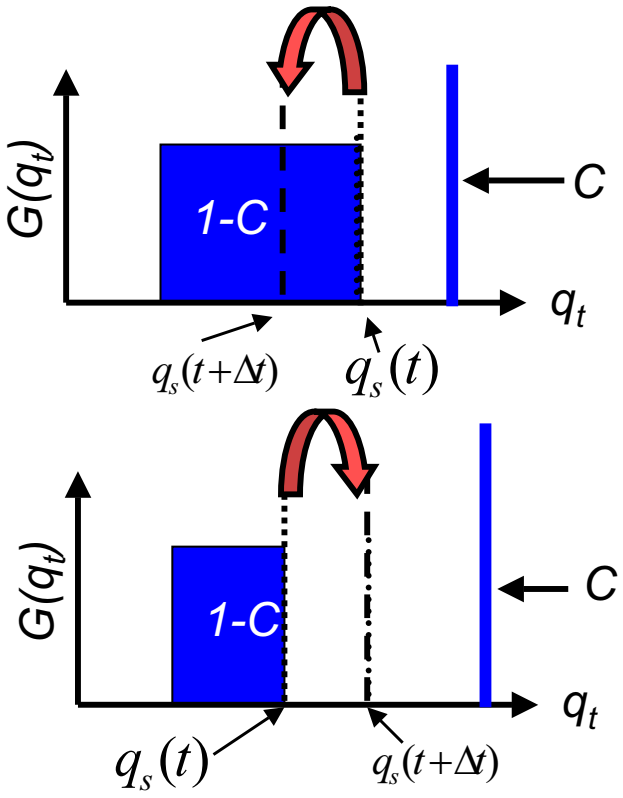

Figure 22: Schematic showing one reversibility issue with Tiedtke scheme. The upper panel shows the impact of a cooling applied to a partially cloudy gridbox. The cooling reduces q_s and thus condenses cloud water, increasing the cloud fraction by the area contained between the dotted and dashed lines. It is assumed no rain is produced and over the subsequent timestep the gridbox is subjected to an equal and opposite warming. One would expect the gridbox should return to the original state, but due to the assumption that the cloud is well mixed and homogeneous, this is not the case (lower panel). The non-reversibility is not necessarily a problem per se; it is consistent with the assumption that the in-cloud homogenization occurs on fast timescales compared to the model timestep. If this were true in the atmosphere then the non-reversibility of the scheme would be realistic. Observations indicate that clouds are far from the homogeneous entities that the Tiedtke cloud scheme and the bulk mass flux convection schemes assume!

know the sub-grid fluctuations of thermodynamic properties.

10 Numerical issues

This lecture now touches briefly on the issue of scheme numerics, and does so since the solution methodology is often omitted from the literature in articles describing cloud schemes. The importance of numerical issues was highlighted by the workshop on *The numerics of physical parametrization* held at ECMWF in 2004. The examples here are taken from the numerics of the Tiedtke (1993) scheme but the comments are valid in general. In fact it should be emphasized that Tiedtke (1993) is one of the rare examples of an article that includes the solution methodology for the prognostic equations implemented.

The Tiedtke (1993) cloud scheme solved the prognostic equation for a generic variable ϕ (cloud water and cloud cover) using an implicit approach (see eqns 27/28 of Beljaars et al., 2004, for details). Sources and sinks are divided into explicit 'slow' processes A_i and implicit 'fast' processes B_i, such that

$$\frac{d\phi}{dt} = A + B\phi. \tag{34}$$

Tiedtke (1993) solves this equation exactly. As some of the parametrizations for B will be complicated, in order to make this solution tractable, each parametrization is approximated by a first order dependence. In other words, if a parametrization were to take the form

$$B_i = \frac{\partial \phi}{\partial t} = K\phi^{\eta}, \tag{35}$$

where η and K are real constants, then solution approximates the tendency by

$$B_i = \frac{\partial \phi}{\partial t} = K\phi\phi_t^{\eta-1}, \tag{36}$$

where ϕ_t is the fixed value of ϕ at the beginning of timestep t. In this way Tiedtke (1993) giving a solution in terms of exponentials (see equations 37 and 38 of that paper)

$$\phi^{t+\Delta t} = \phi_t e^{-B\Delta t} + \frac{A}{B}\left(1 - e^{-B\Delta t}.\right) \tag{37}$$

The special case $F = 0$ has to be treated separately.

To illustrate an example of how the specific solution of an equation set can result in a system very different in practice to that described in the governing equations, we examine the treatment of ice sedimentation that was added to the Tiedtke (1993) scheme and described in Gregory et al. (2000), and was valid until cycle 25r4.

The ice variable was diagnostically divided into two categories of large and small ice particle sizes. The mass mixing ratio of small ice particles, defined as having a dimension less than the threshold of 100 microns ($q_{i<100}$), is given in equation 5 of McFarquhar and Heymsfield (1997), and repeated here for clarity:

$$q_{i<100} = 81.7(\rho q_i)^{0.837} \tag{38}$$

The mass is not allowed to exceed q_i, and the modified constant 81.7 is simply due to the fact that McFarquhar and Heymsfield (1997) use units of gm^{-3}. The large particles are assumed to fall out of a column as snow within one timestep, while the smaller ones are converted to snow if they fall into a clear region or are allowed to sediment to the next layer if it is cloudy (using the maximum-random overlap rules for cloud cover to determine this). The sedimentation fallspeeds for small ice particles are specified according to mass mixing ratio and are given by Heymsfield and Donner (1990).

Although these 'rules' governing the sedimentation of ice appear reasonable, (large-ice particles falling quickly, small ones slowly) closer examination of the original numerical solution method outlined above reveals that the behaviour of the scheme was very different in practice than that intended! The reason was that the implementation set the fall speed of large ice to that required to remove the entire ice contents of a grid-cell to the adjacent cell below, i.e. the speed implied by the CFL criterion. However, the solution was then performed with the exact solution methodology outlined above. The result was that the implied fall speed was actually often lower for large ice than that assumed for small ice, especially at low resolutions that use longer timesteps (see figures 23 and 24). For example, for the T95 model, which uses a one hour timestep, the effective fall speed for large-ice in the upper troposphere is roughly 0.2 m s^{-1}. It is immediately clear why this is unreasonable, since the fallspeeds observed by Heymsfield and Donner (1990) exceed this level even for small ice mass mixing ratios.

Thus alternative numerical approaches are required. Semi-Lagrangian methods to treat the sedimentation/precipitation terms are efficient and can be non-diffusive, are commonly used to achieve numerical accuracy for long timesteps (Leonard, 1991; Wallis and Manson, 1996) and were implemented into the scheme of Lopez (2002). The disadvantage of these methods are the complexity of considering the interaction with other fast processes during the descent. Time splitting is an alternative approach to treat fast processes and fast precipitant fall-speeds. Again the consideration of the interaction with other processes complicates matters; simply handling the sedimentation process itself using shorter sub-timesteps would lead to inaccurate solutions. However, including the consideration of melting, autoconversion and evaporative processes would imply a considerable portion of the cloud physics being run at short timesteps.

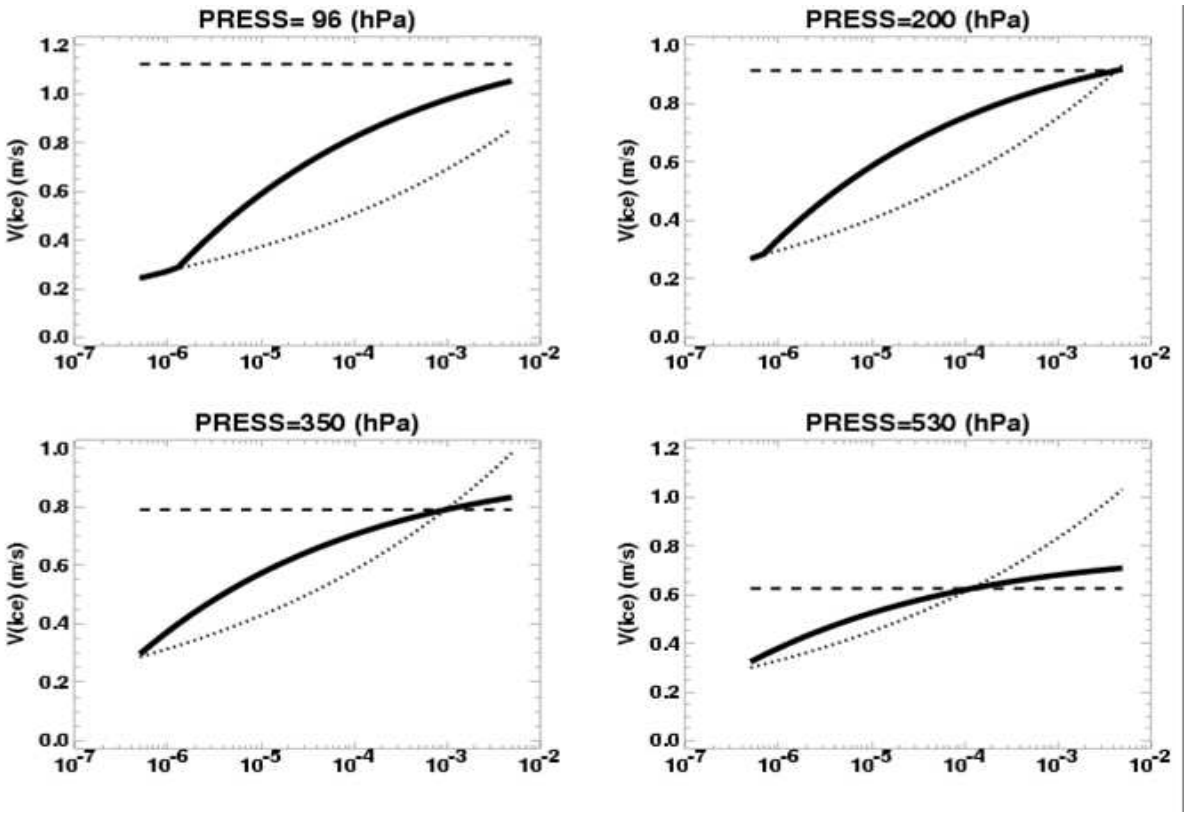

Figure 23: The pre-25r4 model cycle fall speed adopted for small (dot-dash, radius less than 100 microns, function of ice mass mixing ratio), large (dashed, function of resolution and timestep only) and mean (solid) diameter ice particles at various pressure levels. The figure assumes a 900s timestep as used by the T_L511 model and the 60 level vertical grid operational until 2006

Thus in many schemes, and also in the ECMWF model post cycle 25r4, a forward in time, upstream implicit method is applied. If we extend eqn. 34 to include sedimentation/falling/advection at a velocity V

$$\frac{d\phi}{dt} = A + B\phi + \frac{1}{\rho}\frac{d(\rho V \phi)}{dz}, \tag{39}$$

then the upstream forward in time implicit solution is simply:

$$\phi_j^{n+1} = \frac{A\Delta t + \frac{\rho_{z-1}V_{z-1}\phi_{z-1}^{n+1}}{\rho_z \Delta Z}\Delta t + \phi_z^n}{1 + B\Delta t + \frac{\rho_z V_z}{\rho_z \Delta Z}\Delta t} \tag{40}$$

where n is the timelevel and z the vertical coordinate. This is stable, but diffusive for species with fast fall speeds. The use of this scheme greatly reduced the vertical resolution sensitivity of the cloud scheme, as illustrated in fig. 25.

The plan at ECMWF is to generalize this implicit treatment to implement a multi-phase prognostic microphysics scheme, with $m = 5$ prognostic equations for water vapour, cloud liquid water, rain, cloud ice and snow (i.e. the single cloud water equation is replaced by four variables), which leads to a generalized discretization in which the i and j indices refer to the i^th microphysical category :

$$\frac{q_i^{n+1} - q_i^n}{\Delta t} = A_i + \sum_{j=1}^{m} B_{ij} q_j^{n+1} - \sum_{j=1}^{m} B_{ji} q_i^{n+1} + \frac{\rho_{z-1} V_i q_{i,z-1}^{n+1} - \rho V_i q_i^{n+1}}{\rho \Delta Z}. \tag{41}$$

The subscript $z-1$ refers to a term calculated at the model level above the present level z for which all other terms are calculated. The matrix $\widetilde{B}$ represents all the implicit microphysical pathways such that $B_{jk} > 0$ rep-

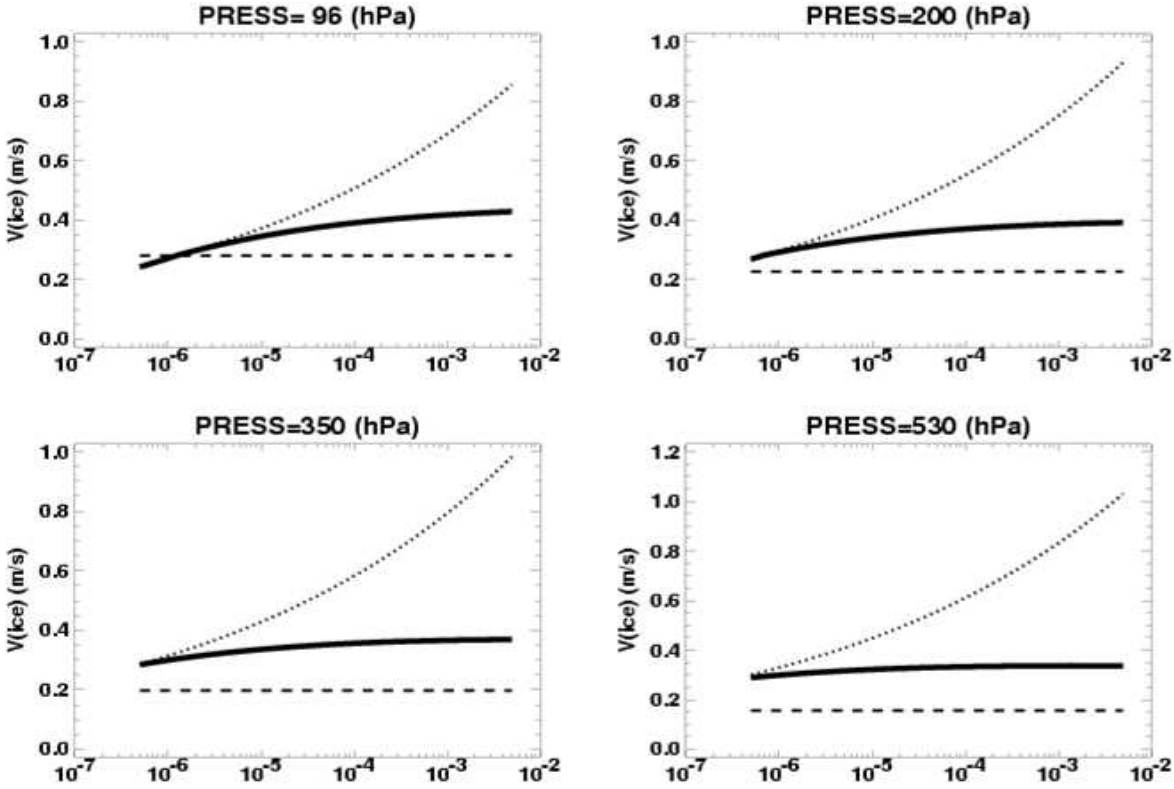

Figure 24: As Fig. 23 but for the 3600s timestep used for the T_L95 resolution model with the same vertical grid.

resents a sink of q_k and a source of q_j. Matrix $\widetilde{B}$ is a positive-definite off the diagonal, with zero diagonal terms since $B_{jj} = 0$ by definition. Some terms, such as the creation of cloud through condensation resulting from adiabatic motion or diabatic heating, are more suitable for an explicit framework, and are retained in the explicit term A.

Due to the cross-terms q_j^{n+1}, eqn. 41 is rearranged to give a straight forward matrix equation. Providing the solution method is robust, the choice for solution is not critical, in contrast to chemical models with typically O(100) species, since in comparison the number of microphysical prognostic equations is small ($m = 5$ in the first instance). The new scheme will use the LU decomposition method (Press et al., 1992). Matters have also been simplified by the fact the advection terms due to convective subsidence (could this be eventually handled in the convection scheme) and sedimentation/falling are all assumed to act in the downward direction, allowing the solution to be conducted level by level from the model top downwards.

The matrix on the left has the microphysical terms in isolation off the diagonal, with the sedimentation term on the diagonal, thus the matrix equation for a 3-variable system is

$$\begin{pmatrix} 1+\Delta t(\frac{V_1}{\Delta z}+B_{21}+B_{31}) & -\Delta t B_{12} & -\Delta t B_{13} \\ -\Delta t B_{21} & 1+\Delta t(\frac{V_2}{\Delta z}+B_{12}+B_{32}) & -\Delta t B_{23} \\ -\Delta t B_{31} & -\Delta t B_{32} & 1+\Delta t(\frac{V_3}{\Delta z}+B_{13}+B_{23}) \end{pmatrix} \cdot \begin{pmatrix} q_1^{n+1} \\ q_2^{n+1} \\ q_3^{n+1} \end{pmatrix} =$$
$$\left[q_1^n + \Delta t \left(A_1 + \frac{\rho_{z-1} V_1 q_{1,z-1}^{n+1}}{\rho \Delta Z} \right), q_2^n + \Delta t \left(A_2 + \frac{\rho_{z-1} V_2 q_{2,z-1}^{n+1}}{\rho \Delta Z} \right), q_3^n + \Delta t \left(A_3 + \frac{\rho_{z-1} V_3 q_{3,z-1}^{n+1}}{\rho \Delta Z} \right) \right]. \quad (42)$$

There are two aspects that require attention. Firstly, although implicit terms are unable to reduce a cloud category to zero, the explicit can, and often will, achieve this. Thus safety checks are required to ensure that all end-of-timestep variables remain positive definite, in addition to ensuring thermodynamic conservation.

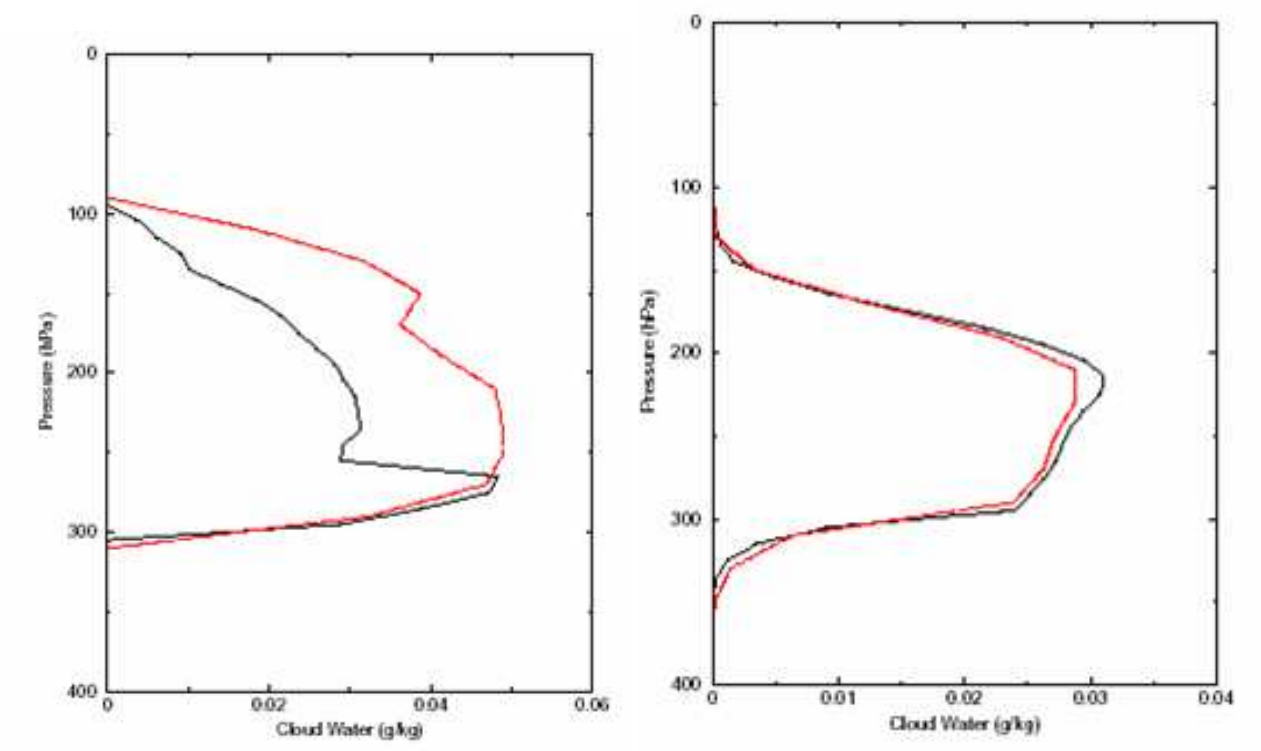

Figure 25: Vertical resolution sensitivity comparing the pre (left) and post (right) 25r4 cloud schemes. Five-day mean profiles of cloud ice water obtained in an idealized cirrus case. An initial cirrus cloud is forced by upper tropospheric ascent, using a 100 layer (Black solid lines) and 50 layer (red dotted lines) vertical grid. Note that the differences in the profiles are due to altered physical processes in the cloud scheme and not the numerical solution procedure, nevertheless, the reduction in vertical resolution sensitivity with the implicit solution is notable.

Secondly, the temperature budget needs to be based on conserved variables when an implicit approach is used; the prototype scheme uses the liquid water temperature T_L defined as:

$$T_L = T - \frac{L_v}{C_p}(q_{liq} + q_{rain}) - \frac{L_s}{C_p}(q_{ice} + q_{snow}). \tag{43}$$

The subscripts are self-explanatory. The temperature change is thus given by

$$\frac{\partial T}{\partial t} = \sum_{j=1}^{m} \frac{L(j)}{C_p}\left(D_{q_j} + \frac{1}{\rho}\frac{\partial}{\partial z}(\rho V_j q_j) + \frac{dq_j}{dt}\right) \tag{44}$$

The second term on the right is the rate of change of species q_j due to *all* processes, including the convective detrainment term D_{q_j} and the advective flux terms, which are included separately since they represent a net T_L flux.

Results from the new five-phase scheme will be presented in a future manuscript.

11 Summary

In summary, this lecture has tried to summarize the various approaches to diagnosing the proportion of a grid box covered by cloud in global models. The main point is that partial coverage can occur if and only if subgrid-scale fluctuations of humidity and temperature exist. All cloud schemes that predict partial cloud cover therefore

implicitly or explicitly make assumptions concerning the magnitude and distribution of these fluctuations; the total water probability density function (PDF).

Simple diagnostic schemes were discussed that use *RH* as their main or only predictor for cloud cover. We then discussed statistical schemes that explicitly specify the humidity PDF. We showed that if the moments of such schemes are time-space invariant, then the cloud cover deriving from statistical schemes can be written as diagnostic *RH* form. In other words, rather than using ad hoc relationships, one can derive a *RH*-scheme to be consistent with an underlying PDF. It was pointed out that knowing the PDF for humidity and cloud fluctuations gives vital extra information that can be used to correct biases in nonlinear processes such as precipitation generation or interaction with radiation.

More complex statistical schemes were then discussed which attempt to predict the sources and sinks of the distribution moments, so that the PDF can realistically respond to the various relevant atmospheric processes. The lecture dwelled on the choice of the prognostic variables, in particular whether it is preferable to predict the PDF moments themselves, or instead to predict integrated and direct cloud quantities such as the cloud liquid water. Advantages and potential drawbacks of each approach were presented. It was pointed out that the Tiedtke scheme is essentially a manifestation of the second approach, where both cloud water *and* cloud cover are predicted, and where often an underlying assumption concerning the humidity and cloud distribution is made to derive the sources and sinks of these prognostic variables.

Future developments of the statistical scheme approach were suggested, including the closure approach for the PDF, and more centrally, the way in which the sources and sinks of the PDF moments due to processes such as convection and microphysics could be derived.

It was finally highlighted that the liquid cloud water variable lends itself to the statistical scheme approach due to the fact that it can be treated as if in suspension and also due to the fast nucleation/evaporation timescales. The same is not true of cloud ice, implying that a hybrid scheme, with cloud ice treated as a separate prognostic variable may be the solution.

Acknowledgments

The author would like to thank ECMWF for their invitation to present at this workshop, and the colleagues at ECMWF who made this work possible over the time the author spent at the centre. The author would like to especially acknowledge Christian Jakob, whose lecture notes on cloud parametrization formed the basis of the author's own lecture series on this subject matter.

References

Barker, H. W., G. L. Stephens, and Q. Fu, 1999: The sensitivity of domain-averaged solar fluxes to assumptions about cloud geometry, *Q. J. R. Meteorol. Soc.*, **125**, 2127–2152.

Barker, H. W., B. A. Wielicki, and L. Parker, 1996: A parameterization for computing grid-averaged solar fluxes for inhomogeneous marine boundary layer clouds. Part II: Validation using satellite data, *J. Atmos. Sci.*, **53**, 2304–2316.

Bechtold, P., J. W. M. Cuijpers, P. Mascart, and P. Trouilhet, 1995: Modeling of trade-wind cumuli with a low-order turbulence model - toward a unified description of Cu and Sc clouds in meteorological models, *J. Atmos. Sci.*, **52**, 455–463.

Bechtold, P., C. Fravalo, and J. P. Pinty, 1992: A model of marine boundary-layer cloudiness for mesoscale applications, *J. Atmos. Sci.*, **49**, 1723–1744.

Beljaars, A., P. Bechtold, M. Köhler, J.-J. Morcrette, A. Tompkins, P. Viterbo, and N. Wedi, 2004: The numerics of physical parametrization, in *Recent developments in numerical methods for atmospheric and ocean modelling*, European Centre for Medium Range Forecasts, Shinfield Park, Reading, UK, pp. 113–134.

Bony, S. and K. A. Emanuel, 2001: A parameterization of the cloudiness associated with cumulus convection: Evaluation using TOGA COARE data, *J. Atmos. Sci.*, **58**, 3158–3183.

Bougeault, P., 1981: Modeling the trade-wind cumulus boundary-layer. Part I: Testing the ensemble cloud relations against numerical data, *J. Atmos. Sci.*, **38**, 2414–2428.

Bougeault, P., 1982: Cloud ensemble relations based on the Gamma probability distribution for the high-order models of the planetary boundary layer, *J. Atmos. Sci.*, **39**, 2691–2700.

Bretherton, C. S. and P. K. Smolarkiewicz, 1989: Gravity waves, compensating subsidence and detrainment around cumulus clouds, *J. Atmos. Sci.*, **46**, 740–759.

Cahalan, R. F., W. Ridgway, and W. J. Wiscombe, 1994: Independent pixel and Monte Carlo estimates of stratocumulus albedo, *J. Atmos. Sci.*, **51**, 3776–3790.

Chaboureau, J. P. and P. Bechtold, 2002: A simple cloud parameterization derived from cloud resolving model data: Diagnostic and prognostic applications, *J. Atmos. Sci.*, **59**, 2362–2372.

Cusack, S., J. M. Edwards, and R. Kershaw, 1999: Estimating the subgrid variance of saturation, and its parametrization for use in a GCM cloud scheme, *Q. J. R. Meteorol. Soc.*, **125**, 3057–3076.

Davis, A., A. Marshak, W. Wiscombe, and R. Cahalan, 1996: Scale invariance of liquid water distributions in marine stratocumulus. Part I: Spectral properties and stationarity issues, *J. Atmos. Sci.*, **53**, 1538–1558.

de Roode, S. R., P. G. Duynkerke, and H. J. J. Jonker, 2004: Large-Eddy Simulation: How Large is Large Enough?, *J. Atmos. Sci.*, **61**(4), 403–421.

Deardorff, J. W., 1974: Three dimensional numerical study of a heated planetary boundary layer, *Bound.-Layer Meteor.*, **7**, 81–106.

Dessler, A. E. and P. Yang, 2003: The distribution of tropical thin cirrus clouds inferred from terra MODIS data, *J. Climate*, **16**, 1241–1247.

Di Giuseppe, F. and A. M. Tompkins, 2003: Effect of spatial organisation on solar radiative transfer in three-dimensional idealized stratocumulus cloud fields, *J. Atmos. Sci.*, **60**, 1774–1794.

Donelan, M. and M. Miyake, 1973: Spectra and fluxes in the boundary layer of the trade-wind zone, *J. Atmos. Sci.*, **30**, 444–464.

Ek, M. and L. Mahrt, 1991: A formulation for boundary-layer cloud cover, *Ann. Geophysicae*, **9**, 716–724.

Emanuel, K. A., 1991: A scheme for representing cumulus convection in large-scale models, *J. Atmos. Sci.*, **48**, 2313–2335.

Fowler, L. D., D. A. Randall, and S. A. Rutledge, 1996: Liquid and ice cloud microphysics in the CSU general circulation model. Part I: Model description and simulated cloud microphysical processes, *J. Climate*, **9**, 489–529.

Fu, Q., B. Carlin, and G. Mace, 2000: Cirrus horizontal inhomogeneity and OLR bias, *Geophys. Res. Lett.*, **27**, 3341–3344.

Gierens, K., 2003: On the transition between heterogeneous and homogeneous freezing, *Atmos. Chem. Phys.*, **3**, 437–446.

Gierens, K., U. Schumann, M. Helten, H. Smit, and P. H. Wang, 2000: Ice-supersaturated regions and subvisible cirrus in the northern midlatitude upper troposphere, *J. Geophys. Res.*, **105**, 22743–22753.

Golaz, J., V. E. Larson, and W. R. Cotton, 2002: A PDF-based parameterization for boundary layer clouds. Part I: Method and model description, *J. Atmos. Sci.*, **59**, 3540–3551.

Gregory, D., J.-J. Morcrette, C. Jakob, A. C. M. Beljaars, and T. Stockdale, 2000: Revision of convection, radiation and cloud schemes in the ECMWF Integrated Forecasting System, *Q. J. R. Meteorol. Soc.*, **126**, 1685–1710.

Gregory, D., D. Wilson, and A. Bushell, 2002: Insights into cloud parametrization provided by a prognostic approach, *Q. J. R. Meteorol. Soc.*, **128**, 1485–1504.

Heymsfield, A. J. and L. J. Donner, 1990: A scheme for parameterizing ice-cloud water content in general circulation models, *J. Atmos. Sci.*, **47**, 1865–1877.

Heymsfield, A. J., R. P. Lawson, and G. W. Sachse, 1998: Growth of ice crystals in a precipitating contrail, *Geophys. Res. lett.*, **25**, 1335–1338.

Heymsfield, A. J. and G. M. McFarquhar, 1996: High albedos of cirrus in the Tropical Pacific Warm Pool: Microphysical interpretations from CEPEX and from Kwajalein, Marshall Islands, *J. Atmos. Sci.*, **53**, 2424–2451.

Hogan, R. J., C. Jakob, and A. J. Illingworth, 2001: Comparison of ECMWF winter-season cloud fraction with radar-derived values, *J. Appl. Meteor.*, **40**, 513–525.

Jakob, C., 2000: *The representation of cloud cover in atmospheric general circulation models*, Ph.D. thesis, University of Munich, Germany, available from ECMWF, Shinfield Park, Reading RG2 9AX, UK.

Kärcher, B. and U. Lohmann, 2002: A parameterization of cirrus cloud formation: Homogeneous freezing of supercooled aerosols, *J. Geophys. Res.*, **107**, DOI: 10.1029/2001JD000470.

Kitchen, M., R. Brown, and A. G. Davies, 1994: Real-time correction of weather radar data for the effects of bright band, range and orographic growth in widespread precipitation, *Q. J. R. Meteorol. Soc.*, **120**, 1231–1254.

Klein, S. A., R. Pincus, C. Hannay, and K.-M. Xu, 2005: Coupling a statistical scheme to a mass flux scheme, *J. Geophys. Res.*, **110**, 10.1029/2004JD005017.

Lappen, C.-L. and D. A. Randall, 2001: Toward a unified parameterization of the boundary layer and moist convection. Part I: A new type of mass-flux model, *J. Atmos. Sci.*, **58**, 2021–2036.

Larson, V. E., 2004: Prognostic equations for cloud fraction and liquid water, and their relation to filtered density functions, *J. Atmos. Sci.*, **61**, 338–351.

Larson, V. E., R. Wood, P. R. Field, J. Golaz, T. H. VonderHaar, and W. R. Cotton, 2001: Small-scale and mesoscale variability of scalars in cloudy boundary layers: One dimensional probability density functions, *J. Atmos. Sci.*, **58**, 1978–1994.

Lenderink, G. and A. P. Siebesma, 2000: Combining the massflux approach with a statistical cloud scheme, in *Proc. 14th Symp. on Boundary Layers and Turbulence*, Amer. Meteor. Soc., Aspen, CO, USA, pp. 66–69.

Leonard, B. P., 1991: The ULTIMATE conservative difference scheme applied to unsteady one-dimensional advection, *Comput. Methods Appl. Mech. Eng.*, **19**, 17–74.

LeTreut, H. and Z. X. Li, 1991: Sensitivity of an atmospheric general circulation model to prescribed SST changes: Feedback effects associated with the simulation of cloud optical properties, *Clim. Dyn.*, **5**, 175–187.

Lewellen, W. S. and S. Yoh, 1993: Binormal model of ensemble partial cloudiness, *J. Atmos. Sci.*, **50**, 1228–1237.

Lohmann, U., N. McFarlane, L. Levkov, K. Abdella, and F. Albers, 1999: Comparing different cloud schemes of a single column model by using mesoscale forcing and nudging technique, *J. Climate*, **12**, 438–461.

Lopez, P., 2002: Implementation and validation of a new prognostic large-scale cloud and precipitation scheme for climate and data-assimilation purposes, *Q. J. R. Meteorol. Soc.*, **128**, 229–257.

Mahrt, L., 1991: Boundary-layer moisture regimes, *Q. J. R. Meteorol. Soc.*, **117**, 151–176.

McFarquhar, G. M. and A. J. Heymsfield, 1997: Parameterization of Tropical Cirrus Ice Crystal Size Distributions and Implications for Radiative Transfer: Results from CEPEX, *J. Atmos. Sci.*, **54**, 2187–2200.

Nishizawa, K., 2000: Parameterization of nonconvective condensation for low-resolution climate models: Comparison of diagnostic schemes for fractional cloud cover and cloud water content, *J. Meteor. Soc. Japan*, **78**, 1–12.

Ose, T., 1993: An examination of the effects of explicit cloud water in the UCLA GCM, *J. Meteor. Soc. Japan*, **71**, 93–109.

Paluch, I. R. and D. H. Lenschow, 1991: Stratiform cloud formation in the marine boundary layer, *J. Atmos. Sci.*, **48**, 2141–2158.

Phelps, G. T. and S. Pond, 1971: Spectra of the temperature and humidity fluctuations and of the fluxes of moisture and sensible heat in the marine Boundary layer, *J. Atmos. Sci.*, **28**, 918–928.

Pincus, R. and S. A. Klein, 2000: Unresolved spatial variability and microphysical process rates in large-scale models, *J. Geophys. Res.*, **105**, 27059–27065.

Pomroy, H. R. and A. J. Illingworth, 2000: Ice cloud inhomogeneity: Quantifying bias in emissivity from radar observations, *Geophys. Res. Lett.*, **27**, 2101–2104.

Press, W. H., S. A. Teukolsky, W. T. Vetterling, and B. P. Flannery, 1992: *Numerical Recipes in Fortran: The Art of Scientific Computing, Second Edition*, Cambridge University Press, pp. 963.

Price, J. D., 2001: A study on boundary layer humidity distributions and errors in parameterised cloud fraction, *Q. J. R. Meteorol. Soc.*, **127**, 739–759.

Price, J. D. and R. Wood, 2002: Comparison of probability density functions for total specific humidity and saturation deficit humidity, and consequences for cloud parametrization, *Q. J. R. Meteorol. Soc.*, **128**, 2059–2072.

Pruppacher, H. R. and J. D. Klett, 1997: *The Microphysics of Clouds and Precipitation*, Kluwer Academic Publishers, pp. 954.

Raymond, D. J. and A. M. Blyth, 1986: A stochastic mixing model for nonprecipitating cumulus clouds, *J. Atmos. Sci.*, **43**, 2708–2718.

Ricard, J. L. and J. F. Royer, 1993: A statistical cloud scheme for use in an AGCM, *Ann. Geophysicae*, **11**, 1095–1115.

Roeckner, E., K. Arpe, L. Bengtsson, M. Christoph, M. Claussen, L. Dümenil, M. Esch, M. Giorgetta, U. Schlese, and U. Schulzweida, 1996: The atmospheric general circulation model ECHAM4: Model description and simulation of present-day climate, Technical Report 218, Max Planck Institute for Meteorology, Bundesstrasse 55, 20146 Hamburg, Germany.

Rotstayn, L. D., 1997: A physically based scheme for the treatment of stratiform precipitation in large-scale models. I: Description and evaluation of the microphysical processes, *Q. J. R. Meteorol. Soc.*, **123**, 1227–1282.

Rotstayn, L. D., 2000: On the ”tuning” of autoconversion parameterizations in climate models, *J. Geophys. Res.*, **105**, 15495–15507.

Slingo, J. M., 1980: A cloud parametrization scheme derived from GATE data for use with a numerical-model, *Q. J. R. Meteorol. Soc.*, **106**, 747–770.

Slingo, J. M., 1987: The development and verification of a cloud prediction scheme for the ECMWF model, *Q. J. R. Meteorol. Soc.*, **113**, 899–927.

Smith, R. N. B., 1990: A scheme for predicting layer clouds and their water-content in a general-circulation model, *Q. J. R. Meteorol. Soc.*, **116**, 435–460.

Spichtinger, P., K. Gierens, and W. Read, 2003: The global distribution of ice-supersaturated regions as seen by the Microwave Limb Sounder, *Q. J. R. Meteorol. Soc.*, **129**, 3391–3410.

Sundqvist, H., E. Berge, and J. E. Kristjansson, 1989: Condensation and cloud parameterization studies with a mesoscale numerical weather prediction model, *Mon. Wea. Rev.*, **117**, 1641–1657.

Tiedtke, M., 1989: A comprehensive mass flux scheme for cumulus parameterization in large-scale models., *Mon. Wea. Rev.*, **117**, 1779–1800.

Tiedtke, M., 1993: Representation of clouds in large-scale models, *Mon. Wea. Rev.*, **121**, 3040–3061.

Tompkins, A. M., 2002: A prognostic parameterization for the subgrid-scale variability of water vapor and clouds in large-scale models and its use to diagnose cloud cover, *J. Atmos. Sci.*, **59**, 1917–1942.

Tompkins, A. M., 2003: Impact of temperature and total water variability on cloud cover assessed using aircraft data, *Q. J. R. Meteorol. Soc.*, **129**, 2151–2170.

Tompkins, A. M., 2005: The parametrization of cloud cover, *ECMWF Moist Processes Lecture Note Series*, p. available at http://www.ecmwf.int/newsevents/training/.

Tompkins, A. M., 2008: A diagnostic parametrization for subgrid-scale temperature variability for use in statistical cloud schemes, *J. Atmos. Sci.*, **66**, manuscript in preparation.

Tompkins, A. M. and J. Berner, 2008: A stochastic convective approach to account for model uncertainty due to unresolved humidity variability, *J. Geophys. Res.*, **113**, doi:10.1029/2007JD009284.

Tompkins, A. M. and K. A. Emanuel, 2000: The vertical resolution sensitivity of simulated equilibrium temperature and water vapour profiles, *Q. J. R. Meteorol. Soc.*, **126**, 1219–1238.

Tompkins, A. M. and M. Janisková, 2004: A cloud scheme for data assimiliation: Description and initial tests, *Q. J. R. Meteorol. Soc.*, **130**, 2495–2518.

Wallis, S. G. and J. R. Manson, 1996: Accurate numerical simulation of advection using large time steps, *Int. J. Num. Meth. Fluids*, **24**, 127–139.

Wang, S. and Q. Wang, 1999: On Condensation and Evaporation in Turbulence Cloud Parameterizations, *J. Atmos. Sci.*, **56**, 3338–3344.

Wielicki, B. A. and L. Parker, 1994: Frequency distributions of cloud liquid water path in oceanic boundary layer cloud as a function of regional cloud fraction, in *Proc. Eighth Conference on Atmospheric Radiation*, Amer. Meteor. Soc., Nashville, TN, USA, pp. 415–417.

Williams, A. G., H. Kraus, and J. M. Hacker, 1996: Transport processes in the tropical warm pool boundary layer. Part I: Spectral composition of fluxes., *J. Atmos. Sci.*, **53**, 1187–1202.

Wood, R. and P. R. Field, 2000: Relationships between total water, condensed water, and cloud fraction in stratiform clouds examined using aircraft data, *J. Atmos. Sci.*, **57**, 1888–1905.

Xu, K.-M. and D. A. Randall, 1996: A semiempirical cloudiness parameterization for use in climate models, *J. Atmos. Sci.*, **53**, 3084–3102.